ARL 65-122
JUNE 1965

Aerospace Research Laboratories

AN ELECTRON BEAM DEVICE FOR REAL GAS FLOW DIAGNOSTICS

S. L. PETRIE
THE OHIO STATE UNIVERSITY
COLUMBUS, OHIO

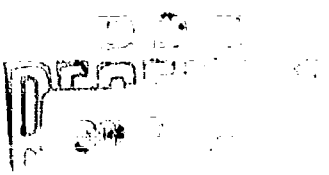

OFFICE OF AEROSPACE RESEARCH

United States Air Force

NOTICES

When Government drawings, specifications, or other data are used for any purpose other than in connection with a definitely related Government procurement operation, the United States Government thereby incurs no responsibility nor any obligation whatsoever; and the fact that the Government may have formulated, furnished, or in any way supplied the said drawings, specifications, or other data, is not to be regarded by implication or otherwise as in any manner licensing the holder or any other person or corporation, or conveying any rights or permission to manufacture, use, or sell any patented invention that may in any way be related thereto.

- - - - - - - - - -

Qualified requesters may obtain copies of this report from the Defense Documentation Center, (DDC), Cameron Station, Alexandria, Virginia.

- - - - - - - - - -

This report has been released to the Office of Technical Services, U. S. Department of Commerce, Washington 25, D. C. for sale to the general public.

- - - - - - - - - -

Copies of ARL Technical Documentary Reports should not be returned to Aerospace Research Laboratories unless return is required by security considerations, contractual obligations or notices on a specified document.

400 - September 1965 - AF33(615)773-S-91

ARL 65-122

AN ELECTRON BEAM DEVICE FOR REAL GAS FLOW DIAGNOSTICS

S. L. PETRIE

AERODYNAMIC LABORATORY
THE OHIO STATE UNIVERSITY
COLUMBUS, OHIO

JUNE 1965

Contract AF 33(657)-11060
Project 7065

AEROSPACE RESEARCH LABORATORIES
OFFICE OF AEROSPACE RESEARCH
UNITED STATES AIR FORCE
WRIGHT-PATTERSON AIR FORCE BASE, OHIO

FOREWORD

This technical report was prepared by S. L. Petrie of the Aerodynamic Laboratory, The Ohio State University, Columbus, Ohio, on Contract AF 33(657)-11060 for the Aerospace Research Laboratories, Office of Aerospace Research, United States Air Force. The work reported herein was accomplished on Project 7065, "Aerospace Simulation Techniques Research." Mr. Emil Walk of the Fluid Dynamics Facilities Laboratory, ARL, served as the technical monitor.

This report has been reviewed and is approved.

ABSTRACT

An electron beam device suitable for use in low density, non-radiating flows is described. It is shown that in certain ranges of gas density the electron beam can be employed to determine the rotational temperature, vibrational temperature and concentration of molecular nitrogen in a high speed air flow. The theoretical analysis required for interpretation of the data obtained with an electron beam is presented and examples of application of the technique are given. Certain design criteria for electron beam generators are discussed.

TABLE OF CONTENTS

Section		Page
I	INTRODUCTION	1
II	THE ELECTRON BEAM GENERATOR	2
III	INTERPRETATION OF BEAM-INDUCED EMISSION	4
	A. General Considerations	4
	B. Excitation-Emission Process	6
	C. Rotational Temperature	7
	D. Vibrational Temperature	10
	E. Number Density	11
IV	EXPERIMENTAL PROCEDURES	13
	A. Rotational Temperature	13
	B. Vibrational Temperature	15
	C. Number Density	17
V	SUMMARY AND CONCLUSION	18
	REFERENCES	20

LIST OF ILLUSTRATIONS

Figure		Page
1	Electron Beam Schematic	24
2	Electron Beam Vacuum System Performance	25
3	Electron Gun Schematic	26
4	Gun Mount Details	27
5	Electron Beam Generators	28
6	Beam-Wind Tunnel Assembly	29
7	Partial Energy Level Diagram for N_2 and N_2^+	30
8	Iso-Intensity Plot for (0,0) Band of N_2^+ First Negative Emission; T_R vs. K_2	31
9	Iso-Intensity Plot for (0,0) Band of N_2^+ First Negative Emission; T_R vs. K_1	32
10	Band Intensity Ratios for N_2^+ First Negative Emission System	33
11	N_2^+ (0,2) Band Intensity Slope Ratio as a Function of Vibrational Temperature	34
12	$K' = 11$ Line Intensity Slope Ratio as a Function of Rotational Temperature	35
13	Typical Spectrogram from 3-meter Grating Spectrograph	36
14	Densitometer Recording for N_2^+ (0,0) Band	37
15	Typical Emulsion Calibration Curve	38
16	Line-Slope Plot for N_2^+ (0,0) Band	39
17	Typical Spectrogram from f/5 Prism Spectrograph	40
18	Densitometer Trace of N_2^+ (0,2) Band	41
19	$K' = 11$ Line Intensity in N_2^+ (0,0) Band	42
20	N_2^+ (0,0) Band Intensity Determined with a Photomultiplier	43
21	N_2^+ (0,2) and N_2^+ (1,2) Band Intensities Determined with f/5 Prism Spectrograph	44

LIST OF TABLES

Table		Page
1	Typical Line Intensities for N_2^+ (0,0) Band	14
2	N_2 Vibrational Temperature Determined with an Electron Beam	16
3	Values of $Log_{10}[(G)\nu^4/\nu_o^4]$ for Various Rotational Temperatures	21
4	N_2^+ First Negative Bands	21
5	Relative Transition Probabilities $p(v',v'') = R_e^2 q(v',v'')$ for Transitions $N_2^+B^2\Sigma \rightarrow N_2^+X^2\Sigma$	22
6	Franck-Condon Factors for Transition $N_2^+B^2\Sigma \rightarrow N_2^+X^2\Sigma$	22
7	Franck-Condon Factors for Transition $N_2X^1\Sigma \rightarrow N_2^+B^2\Sigma$	22
8	Relative Populations of N_2 Vibrational Energy Levels, $e^{-G_o(v_o)hc/kT}$	23

LIST OF SYMBOLS

a	Rate of photon emission
c	Speed of light
C_1	Intensity constant, Eq. (8)
C_2	Intensity constant, Eq. (12)
e	Electron
f	Intensity function, Eq. (13)
G	Vibrational term value
G_o	Relative vibrational term value
(G)	Rotational temperature function, Eq. (4)
H	Line intensity function, Eq. (2)
h	Planck's constant
I	Intensity
I_o	Intensity constant, Eq. (4)
I_o'	Intensity constant, Eq. (3)
K	Rotational quantum number
k	Boltzmann's constant
N_{N_2}	N_2 number density
$N_2X^1\Sigma$	Ground electronic energy level of N_2
$N_2^+X^2\Sigma$	Ground electronic energy level of N_2^+
$N_2^+B^2\Sigma$	Excited electronic energy level of N_2^+
$p(v',v_o)$	Vibrational transition probability for $N_2X^1\Sigma \rightarrow N_2^+B^2\Sigma$
$p(v',v'')$	Vibrational transition probability for $N_2^+B^2\Sigma \rightarrow N_2^+X^2\Sigma$
$P(K',K'')$	Rotational transition probability for $N_2^+B^2\Sigma \rightarrow N_2^+X^2\Sigma$
$q(v',v_o)$	Franck-Condon Factor for $N_2X^1\Sigma \rightarrow N_2^+B^2\Sigma$

LIST OF SYMBOLS (Continued)

$q(v',v'')$	Franck-Condon Factor for $N_2^+B^2\Sigma \rightarrow N_2^+X^2\Sigma$
Q	Partition function (state sum)
R	Rotational slope function
S	Vibrational slope function
T	Temperature
v	Vibrational quantum number
θ	Characteristic rotational temperature (2.891°K for N_2)
ν	Wave number
ν_o	Reference wave number

Subscripts

c	Calibration conditions
N_2^+	Conditions for N_2^+ first negative emission system
O	Conditions in N_2 ground electronic state
R,ROT	Conditions for rotational energy mode
V,VIB	Conditions for vibrational energy mode

Superscripts

'	Conditions in $N_2^+B^2\Sigma$ state
"	Conditions in $N_2^+X^2\Sigma$ state

I. INTRODUCTION

Laboratory simulation of flow fields with wind tunnels long has been an established technique. New facilities continually have been developed to extend the speed and altitude ranges which can be simulated. Although the technology of facility design has advanced at a rapid rate, there has been a sizeable lag in the development of adequate flow calibration devices.

The diagnostic procedures for advanced test devices are complicated by the presence of non-equilibrium effects in the effluent. For example, in a high enthalpy wind tunnel, dissociation and ionization of the gas occur, and as the gas expands through the nozzle, chemical recombination and thermodynamic relaxation take place. Since recombination and relaxation are rate processes, they are coupled strongly to the gasdynamic features of the flow. Thus, there is a direct relationship between the local flow velocity and the degrees of recombination and relaxation with the possible existence of non-equilibrium effects. Similarly, in very low density facilities, non-equilibrium in the thermodynamic relaxation processes may occur and viscous effects can become predominant. Non-equilibrium behavior and viscous effects both destroy the simple relationships used to interpret conventional calibration data and necessitate a much larger number of independent measurements to determine the state of the effluent.

The calibration items of interest for a test facility can be grouped into three main categories: (1) those associated with the gasdynamic state, (2) those describing the chemical nature of the effluent, and (3) the variables specifying the local thermodynamic state. Various types of probes have been proposed for determining certain features of the flow. However, to obtain a direct measurement of the detailed chemical composition and/or the thermodynamic state of the effluent, spectroscopic methods generally must be applied.

Although tedious, spectroscopic techniques are particularly attractive since they can be employed without causing any disturbance in the gas during the time of measurement. Both emission and absorption spectroscopy can be considered for application. However, in highly expanded flows, the gas temperatures and pressures generally are so low (even in arc-heated wind tunnels) that the gas does not emit nor absorb a sufficient amount of radiation for quantitative measurements. In some instances, non-thermal excitation of the gas may be present[1] allowing the application of conventional spectrographic techniques, but usually this is not the case. Hence, to allow the application of spectroscopic techniques to highly expanded non-radiating flows, various methods for causing the test gas to emit radiation were examined.

It would be possible to excite the gas with alpha particles, beta particles, or x-rays. However, the difficulties with obtaining well

Manuscript released by the author 3 June 1965 for publication as an ARL Technical Report.

collimated beams, the requirements for adequate shielding from the x-rays, and the resultant contamination of the test facility associated with these techniques make them undesirable. Previous theoretical and experimental studies by Gadamer[2] and Muntz[3] directed towards the measurement of gas properties with an electron beam in low density, non-radiating flows were encouraging. In this technique, a narrow beam of electrons is projected across the flow and the interaction of the electrons with the gas particles produces a column of radiating gas coincident with the beam. Spectroscopic analysis of the radiation yields a direct measurement of the rotational and vibrational temperatures and concentrations of the active species at arbitrary locations within the test gas.

Analysis of the spectrum induced by an electron beam passing through nitrogen has been given by Muntz.[3] The applicability of the technique in high speed flows of arc-heated air has been demonstrated by Petrie, Pierce and Fishburne.[4] In Ref. 4, data from the electron beam were compared with conventional calibration data and various theoretical predictions to deduce the thermo-chemical properties of the effluent generated by an arc-heated wind tunnel.

The electron beam has proven to be an extremely useful diagnostic device. It can be applied to any low density flow to give a direct measurement of temperature and species concentration without altering the basic energy content of the medium under investigation. The purpose of this report is to summarize the theoretical information required to interpret the spectral data obtained with an electron beam and to present the pertinent design criterion for a suitable electron beam generator. Detailed descriptions of the application of the beam technique in wind tunnel diagnostics may be found in Ref. 4.

II. THE ELECTRON BEAM GENERATOR

The studies reported in Refs. 2 and 3 indicate that sufficient radiation can be obtained from an electron beam passing through nitrogen with beam currents in the range of 10 to 200 microamperes and beam voltages from 10 to 20 kilovolts. The high voltage is utilized to reduce spreading of the beam due to elastic collisions between beam electrons and gas particles. The beam is projected completely across the test flow as shown in Fig. 1 and profiles of gas properties can be obtained by examining various points along the length of the beam. Because of the high speed of the electrons within the beam, a gas flow has little effect on the beam shape or its path through the flow. A narrow beam (1 mm diameter) is employed to obtain good spatial resolution.

An electron beam with the desired current and voltage can be obtained from electron guns used in commercial television picture tubes. These TV guns are attractive because they are readily available at low cost

($2.00 each). However, commercially available electron guns usually have oxide-coated cathodes which easily become contaminated if operated at pressures much above 10^{-4} mm Hg. Hence, to project an electron beam across a flow with a static pressure above 10^{-4} mm Hg, an orifice through which the accelerated electrons can pass freely into the test region must separate the electron gun from the test gas and a dynamic pumping system must be employed to maintain the gun at a pressure below 10^{-4} mm Hg.

The electron beam system described here was designed to operate with static pressures (at room temperature) up to 500 μ Hg. The beam vacuum system consists of a six-inch, four-stage oil diffusion pump with an unbaffled pumping speed of 1520 liters/second at pressures from 3×10^{-8} to 5×10^{-3} mm Hg. A water-cooled baffle is employed between the gun chamber and the oil diffusion pump to reduce "backstreaming" of the pump vapors into the gun chamber. The performance of the vacuum system is shown graphically in Fig. 2 where it can be seen that the gun chamber pressure is maintained at the desired level with external pressures up to 500 μ Hg.

Electron gun types 19BWP4 and 21CPB4 have been employed with the 19BWP4 displaying the longer lifetime. The 19BWP4 gun is a 114° magnetic deflection, electrostatic focus type with an ultor voltage range from 12 to 23.5 kv and a rated cathode heater voltage of 6.3 volts. Voltages are supplied to the gun by a standard high voltage power supply with an adjustable output up to 30 kv at a maximum current of three milliamperes. The heater, cathode, and grids are placed at high negative voltages with respect to ground potential. Variable grid voltages are obtained by leaking current to ground through adjustable resistors and milliammeters are used in all grid circuits to monitor the gun performance. Cathode heater currents are supplied by a high voltage transformer and normal operation of a gun usually requires heater currents as much as 50% above the rated current of 450 milliamperes. The net beam current passing through the test gas is measured with a microampmeter. A schematic diagram of the electrical system is given in Fig. 3.

Other investigators[3,5] experienced difficulties in operating guns with oxide-coated cathodes in continuously pumped vacuum systems. These difficulties were caused principally by decomposition of silicone vapor from the oil diffusion pump on the cathode surface causing erratic variations of the beam current. With Consolidated Vacuum Corporation Convoil 20 pump fluid, no difficulties with cathode contamination have been experienced with the gun system described here.

A rather marked degradation in gun performance has been noticed each time the pressure in the gun chamber is brought to atmospheric pressure. After each exposure to atmospheric pressure, an increase in the cathode heater current is required to obtain a given value of the cathode current. Much more satisfactory performance and longer gun life could be obtained by continually maintaining the gun at a low pressure.

The electron guns are mounted in a pyrex tube which is held in place in the gun chamber by a ball-and-socket arrangement shown in Fig. 4. The ball-and-socket allows mechanical alignment of the gun axis with the exit orifice. To obtain precise alignment of the gun, and, hence, maximum beam current, a small permanent magnet (300 gauss) with a movable pole-piece is placed around the electron gun in the region of the gun cathode. After initially positioning the gun with the ball-and-socket, final alignment of the beam can be accomplished simply by moving the magnet pole-piece.

The electron beam is extremely sensitive to changes in the ambient magnetic field strength. In applications of the beam in arc-heated wind tunnels, the magnetic fields generated by the arc-heater have been found of sufficient strength to substantially alter the position of the beam. Any small deflection of the beam upstream of the exit orifice will result in a large reduction of the beam current passing through the test flow. To eliminate this deflection, it is advisable that shielding be employed in the gun chamber. Further, a second permanent magnet can be employed near the exit orifice so that minor changes in the ambient field strength result in extremely small percentage changes in the field acting on the beam. Additional benefits can be obtained with this orifice magnet. The converging magnetic field near the orifice refocusses the beam and allows much higher currents to be projected through the orifice and across the flow. The two magnets are shown in the schematic diagram of Fig. 1.

Photographs of two electron beam systems are given in Fig. 5. Beam systems connected to test facilities are shown in Fig. 6. The mechanical configuration for the beam generators shown here was chosen so that the generators could be moved easily from one test facility to another. More compact designs could be employed if this type of flexibility is not required.

III. INTERPRETATION OF BEAM-INDUCED EMISSION

A. GENERAL CONSIDERATIONS

The validity of the measurements obtained with an electron beam depends upon a thorough understanding of the excitation-emission processes which occur within the beam. This must include a consideration of the effects of the beam on the basic energy content of the gas. It is shown that in certain ranges of gas density, the vibrational and rotational fine structures of the emitted radiation may be used to determine the vibrational and rotational temperatures of the active molecules and that the intensity of the radiation may be related directly to the density of the radiating species.

When a beam of high energy electrons passes through a gas, the electrons collide with gas particles. The collisions may be elastic or inelastic, depending upon the total kinetic energy of the interacting pair after the collision. The elastic collisions contribute primarily to the spreading of the beam while the inelastic collisions result in radiation by the excited particles.

During an elastic collision, the total kinetic energy of the interacting particles is conserved. The electrons are scattered by the heavy gas particles and a portion of the electronic energy may be transferred to the gas particles causing an increase in the static temperature of the gas.

In an inelastic collision, the high speed electron imparts a certain portion of its kinetic energy to the internal energy of the heavy particle. This energy appears principally as electronic excitation of the heavy gas particles. After electronic excitation, the excited particle may emit radiation during a spontaneous transition to its ground electronic state, or it may collide with another particle during the lifetime of the excited state, giving up the excess energy to the kinetic energy of the interacting pair. The latter process is called collision quenching.

The emission of light due to a spontaneous transition does not contribute to the general energy level of the gas but passes out of the system with little attenuation. It is precisely this radiation which is analyzed to determine the properties of the test gas. Only in the special case that the radiation results from a resonant transition could self-absorption by the gas present difficulties in interpretation of the radiation.

In addition to these direct modes of transfer of electron beam energy, other processes can be important. When a particle is struck by a beam electron, ionization of the particle may occur so that the radiative transition actually connects an excited state of the ion with the ion's ground electronic state (see Section III-B). Such is true for nitrogen. In this case, the radiative transitions leave the ions in their ground electronic state and recombination of the ions with electrons can occur in the body of the gas. Each recombination can contribute energy equal to the ionization potential of the particle to the kinetic energy of the gas. In addition, secondary electrons freed by ionization of the particle can add energy to the gas by elastic collisions or may electronically excite other gas particles. The presence of ions as well as particles in metastable electronic energy states can lead to "afterglow" in a flowing gas, which could be particularly bothersome if the total radiated light were employed for denisty measurements.

It should be evident from the above discussions that certain limits on the range of gas density exist for applicability of the electron beam technique. At very low densities, there are an insufficient number of gas particles to be excited by the beam so that little radiation is observed. The admissible minimum density purely is a function of the

sensitivity of the detecting equipment. At very high densities, the collision frequencies between electrons and gas particles as well as between gas particles increases to a point where two phenomena may occur. First, the number of elastic collisions which the electrons experience may increase so that there is a large amount of scattering of the beam electrons with attendant losses in spatial resolution and intensity. Second, the number of collisions between electronically excited and unexcited particles can increase so that collision quenching becomes important. As discussed in the following section, the theoretical interpretation of the beam-induced radiation is developed with the assumption that there is no collision quenching. Hence, the analysis employed to obtain temperatures and particle densities may be invalidated at high densities.

In addition to the limits on gas density, certain bounds must be placed upon the value of the beam voltage employed. If very high voltages are used, the collision cross-section of beam electrons with gas particles decreases to a point where little excitation may result, and, hence, the radiation intensity may be reduced to an unacceptable low value. With very low beam voltages, the electron collision cross section may become so large that the elastic scattering of the electrons becomes a problem.

The complexity of the many processes which occur during excitation of a gas by an electron beam make an accurate theoretical analysis of the over-all energy addition process difficult. In Ref. 4, the results of detailed experimental studies aimed at determining the amount of energy added to air by an electron beam are reported. It is shown that no measurable increase of the gas temperature occurs for air densities up to that corresponding to a pressure of 400 μ Hg at room temperature with beam voltages from 10 to 20 kilovolts. The pressure of 400 μ Hg was the maximum value which could be examined in Ref. 4 and should not be taken as the maximum permissible value for application of the technique. The reader is referred to Ref. 4 for further details.

B. EXCITATION-EMISSION PROCESS

When the electron beam is passed through air, the predominant radiation observed is due to the first negative emission system of the ionized nitrogen molecule (N_2^+) and the first and second positive systems of the unionized nitrogen molecule (N_2). Except for the very intense (0,0) band of the N_2^+ radiation at 3914 Å, the first negative and second positive bands appear with nearly equal intensities and the first positive system appears only weakly. Spectra from other species present in heated air (NO, O_2, O) and from A, H_e, and CO_2 have been observed[6] but with intensities much less than that of the (0,0) band of N_2^+ radiation. In the following, reference is made only to the properties of diatomic nitrogen. Since detailed analyses of the excitation-emission process are given in Refs. 3 and 4, only a summary of the theory will be given here.

The electronic transition comprising the N_2^+ first negative emission system is denoted by $N_2^+B^2\Sigma \rightarrow N_2^+X^2\Sigma$. The transitions giving rise to the observed radiation are shown in the energy level diagram of Fig. 7. The emission is excited by collisions between electrons and nitrogen molecules in the ground state ($N_2X^1\Sigma$). The excitation transition is denoted by $N_2X^1\Sigma \rightarrow N_2^+B^2\Sigma$ and is shown in Fig. 7. This excitation-emission process can be represented symbolically as

$$N_2X^1\Sigma + e \rightarrow N_2^+B^2\Sigma + 2e$$
$$\hookrightarrow N_2^+X^2\Sigma + h\nu$$

The analyses of Refs. 3 and 4 substantiate the assumed excitation process so that other possible ways by which the $N_2^+B^2\Sigma$ state can be populated may be ignored. Also note that collision quenching of the $N_2^+B^2\Sigma$ state is neglected.

In specifying a detailed model for the excitation-emission process, several simplifying assumptions are employed. It is assumed that the population in the N_2 ground state can be represented by effective rotational and vibrational temperatures. That is, Boltzmann population distributions are assumed. It is not necessary that the rotational and vibrational temperatures be equal. In fact, arbitrary population distributions may be assumed for each mode so long as some expression for the population in the N_2 ground state is available. The transition probabilities describing the excitation and radiative transitions between vibrational energy levels are assumed to be given in terms of the Franck-Condon factors (or the squares of the overlap integrals). Since the excitation is due to high speed electrons, the duration of time for the excitation should be small so that the relative positons of the nuclei is the N_2 molecule should not change during excitation. This is the condition which must be fulfilled for applicability of the Franck-Condon principle. The radiative transition is a spontaneous emission process and the Franck-Condon principle should apply directly. The probabilities for transitions between the rotational energy levels are assumed equal to the corresponding values for usual optical transitions.

C. ROTATIONAL TEMPERATURE

The intensity of a particular rotational line in the emission is given by the product of the rate of photon emission and the energy of the photon. Hence,

$$(I_{K',K''})_{v',v''} = (a_{K',K''})_{v',v''} hc(\nu_{K',K''})_{v',v''} \qquad (1)$$

where $(I_{K',K''})_{v',v''}$ is the intensity of the rotational line arising from

the transition from the K' rotational level within the v' vibrational level in the $N_2^+B^2\Sigma$ state to the K" rotational level within the v" vibrational level in the $N_2^+X^2\Sigma$ state, $(a_{K',K"})_{v',v"}$ is the rate of photon emission for the transition, and $(\nu_{K',K"})_{v',v"}$ is the wave number (inverse wavelength) of the transition. The expression for the rate of photon emission is obtained from the detailed analysis of the excitation-emission process with the assumptions discussed above. The final result for the line intensity is[4]

$$(I_{K',K"})_{v',v"} \propto (\nu_{K',K"})^4_{v',v"} \frac{N_{N_2}}{Q_{VIB}} q(v',v")P(K'K") \times \sum_{v_o} q(v',v_o) \frac{H(v_o,K',T_R)}{Q_{ROT}} e^{-G(v_o)hc/kT_V} \quad (2)$$

where N_{N_2} is the number density of nitrogen molecules in the N_2 ground electronic energy state, Q_{VIB} and Q_{ROT} are vibrational and rotational partition functions, $q(v',v")$ and $q(v',v_o)$ are the Franck-Condon factors for the emission and excitation, respectively, $P(K',K")$ is the rotational transition probability for the emission, $G(v_o)$ is the term value for the v_o vibrational level, T_R and T_V are the rotational and vibrational temperatures, and $H(v_o,K',T_R)$ is a known function of the indicated variables.

In the observed emission, the rotational lines for which $v'=v"=0$ (the 0,0 band) are much more intense than the lines of other bands. In the (0,0) band, two branches of lines appear. The P-branch lines are very close together and form the band head while the R-branch lines are farther apart and can be separated by a spectrograph with moderate dispersion. When equation (2) is written for the R-branch lines and the dependency of the rotational energy on the vibrational quantum number is ignored, the intensity of a particular R-branch line is[4]

$$\frac{I_{K',K"}/I_o'}{K'(G)\nu^4_{K',K"}/\nu_o^4} = \frac{N_{N_2}}{Q_{VIB}} \left[\sum_{v_o} q(0,v_o)e^{-G(v_o)hc/kT_V} \right] \frac{e^{-K'(K'+1)\theta/T_R}}{Q_{ROT}} \quad (3)$$

where I_o' is a constant, ν_o is a reference wave number, $\theta = 2.891^oK$, and (G) is given as

$$(G) = \frac{1}{2K'+1} \left[(K'+1)e^{-2(K'+1)\theta/T_R} + K'e^{+2K'\theta/T_R} \right]$$

For given vibrational and rotational temperatures, the factors multiplying the exponential are constants independent of K'. Hence, equation (3) can be written as

$$\frac{I_{K',K''}/I_o}{K'(G)\nu^4_{K',K''}/\nu_o^4} = e^{-K'(K'+1)\theta/T_R} \tag{4}$$

The rotational temperature of the nitrogen molecules in the N_2 ground electronic state can be determined by measuring the relative intensities of the rotational lines in the R-branch and plotting $\ln[(I_{K',K''}/I_o)/K'(G)\nu_{K',K''}/\nu_o^4]$ against $K'(K'+1)$. This plot will produce a straight line with a slope of $-\theta/T_R$. Since (G) is a function of both K' and T_R, an iterative procedure of solution is required. A value of T_R is assumed and the graph is plotted giving a new value of T_R and the iteration is repeated. The values of $\log [(G)\nu_{K'^4,K''}/\nu_o^4]$ are given in Table 3 where it is seen that the variation of $\log [(G)\nu_{K'^4,K''}/\nu_o^4]$ with T_R is slow so that the iteration converges rapidly. A sample calculation of T_R by this method is given in Section IV.

An iso-intensity method of rotational temperature determination can be applied with the intensity expression given by equation (4). Let K_1' and K_2' be the rotational quantum numbers in the $N_2^+B^2\Sigma$ state for two lines which have the same intensity. Then the rotational temperature is obtained from equation (4) as

$$T_R = \frac{K_2'(K_2'+1) - K_1'(K_1'+1)}{\ln[K_2'(G)_2\nu_2^4/\nu_o^4] - \ln[K_1'(G)_1\nu_1^4/\nu_o^4]}\,\theta \tag{5}$$

The need for an iterative solution for the rotational temperature now can be eliminated by referring to the plots shown in Figs. 8 and 9. The rotational temperature can be determined by measuring the relative intensities of the rotational lines and finding the values of $K'(K_1'$ and $K_2')$ which correspond to lines of equal intensity. The temperature then is obtained directly from Figs. 8 and 9. However, care must be exercised when the iso-intensity method is applied. At high rotational temperatures (greater than 800°K), lines from the P-branch in the (0,0) band interfere with the first few lines in the R-branch. These R-branch lines appear with intensities which are too high and errors in the temperature result. The iso-intensity method is convenient for "quick" answers since no calibration of the detecting equipment (particularly photographic plates) is required; however, greatest accuracy is obtained by plotting the intensity function against $K'(K'+1)$.

It is important to realize that the rotational temperature determined with the above techniques is that of the unionized nitrogen molecules in the ground electronic state-that is, the temperature of the molecules

before excitation by the electron beam. Since the rotational energy mode requires only a few inter-molecular collisions (approximately 10) to become equilibrated with the translational energy mode, the rotational and static temperatures of the gas should be equal in most cases of interest. However, the possibility of rotational non-equilibrium should be ascertained in any application of the electron beam technique.

D. VIBRATIONAL TEMPERATURE

The intensity of a particular band in the N_2^+ emission is derived in the same manner as discussed in the previous section. Obviously, the rotational structure of the band is not considered. The result is[4]

$$I_{v',v''} \propto \frac{N_{N_2}}{Q_{VIB}} \nu^4_{v',v''} \, q(v',v'') \sum_{v_o} q(v',v_o) e^{-G_o(v_o)hc/kT_V} \qquad (6)$$

The vibrational temperature is determined from equation (6) by expressing the ratio of intensities of two bands in the form

$$\frac{I_{v_1',v_1''}}{I_{v_2',v_2''}} = \left(\frac{\nu_{v_1',v_1''}}{\nu_{v_2',v_2''}} \right)^4 \frac{q(v_1',v_1'')}{q(v_2',v_2'')} \frac{\sum_{v_o} q(v_1',v_o) e^{-G_o(v_o)hc/kT_V}}{\sum_{v_o} q(v_2',v_o) e^{-G_o(v_o)hc/kT_V}} \qquad (7)$$

When the electron beam is passed through air, the (0,2), (1,3), (2,4), (0,1), (1,2) and (2,3) bands are suitable for vibrational temperature determinations. The wavelengths of these bands are given in Table 4. The (0,0) band at 3914 Å usually is too intense for quantitative purpose when the sensitivity of the detection system is adjusted to give reasonable values for the other band intensities. The bands in the (1,0) progression near 3580 Å are overlapped by the (0,1) band of the N_2 second positive emission system.

From equation (7), the ratio of intensities of two bands in the emission is a function only of the vibrational temperature of the N_2 molecules in the ground electronic state ($N_2X^1\Sigma$). The ratios of intensities for various band combinations are shown as a function of N_2 vibrational temperature in Fig. 10 where it is seen that reasonable sensitivity is obtained for temperatures from 1000°K to 3000°K. Thus, the vibrational temperature of the N_2 molecules may be determined by measuring the intensities of the bands in the emission and consulting the curves of Fig. 10. To allow computations of band intensity ratios of interest not given in Fig. 10, the Franck-Condon factors, $q(v',v'')$ and $q(v',v_o)$ are given in Tables 5, 6 and 7 and the Boltzmann factor, $e^{-G_o(v_o)hc/kT_V}$, is given in Table 8 as a function of the vibrational quantum number and vibrational temperature. As example of vibrational temperature determination is given in Section IV.

E. NUMBER DENSITY

Various methods exist for the measurement of the number density of nitrogen with an electron beam. Any of the following means may be employed:

(1) measurement of the intensity of a particular rotational line in a vibration-rotation band,

(2) measurement of the intensity of a band, or

(3) measurement of the total radiation intensity.

In certain cases, one method is more advisable than others.

The intensity of a given rotational line in the N_2^+ emission is given by equation (2). For a particular line, the transition probabilities and the wave number of the line are independent of the number density, vibrational temperature, and rotational temperature. With this in mind, equation (2) is re-written as[4]

$$I_{K',K''} = C_1 \left[\sum_{v_o} \frac{q(v',v_o)}{Q_{VIB}} e^{-G_o(v_o)hc/kT_V} \right] \left[\frac{K'+1}{Q_{ROT}} e^{-(K'+1)(K'+2)\theta/T_R} + \frac{K'}{Q_{ROT}} e^{-K'(K'-1)\theta/T_R} \right] N_{N_2} \tag{8}$$

where C_1 includes the transition probabilities and constant of proportionality in equation (2) and $H(v_o,K',T_R)$ has been written in explicit form ignoring the effect of vibration on the rotational energy mode. Equation (8) shows that the intensity of a given line varies linearly with the N_2 number density with a slope dependent upon both the rotational and vibrational temperatures. Equation (8) is re-written in a more convenient form by defining the quantities $S(T_V)$ and $R(T_R)$ as

$$S(T_V) = \sum_{v_o} \frac{q(v',v_o)}{Q_{VIB}} e^{-G_o(v_o)hc/kT_V} \tag{9}$$

$$R(T_R) = \left[\frac{K'+1}{Q_{ROT}} e^{-(K'+1)(K'+2)\theta/T_R} + \frac{K'}{Q_{ROT}} e^{-K'(K'-1)\theta/T_R} \right] \tag{10}$$

Thus,

$$I_{K',K''} = \left[\frac{S(T_V)}{S(T_c)} \right] \left[\frac{R(T_R)}{R(T_c)} \right] [C_1 S(T_c) R(T_c)] N_{N_2} \qquad (11)$$

where $S(T_c)$ and $R(T_c)$ are the functions defined in equations (9) and (10) evaluated at a known calibration temperature (room temperature). Typical values of the slope ratios $S(T_V)/S(T_c)$ and $R(T_R)/R(T_c)$ are shown graphically in Figs. 11 and 12.

To determine the nitrogen number density from the measurement of a line intensity, a room temperature calibration must be performed to determine the factor $[C_1 S(T_c) R(T_c)]$. The constant C_1 includes not only the quantities indicated by equation (8), but also the sensitivity of the measuring system. The vibrational and rotational temperatures are measured in the test gas and the slope ratios $S(T_V)/S(T_c)$ and $R(T_R)/R(T_c)$ are determined from Figs. 11 and 12 (perhaps re-drawn for a different line or band). The N_2 number density then is determined with the measured line intensity and equation (11). Additional details of the procedures are given in the examples of Section IV.

The N_2 number density also can be determined by measuring the intensity of a particular band. For a given band, equation (6) can be written as

$$I_{v',v''} = \left[\frac{S(T_V)}{S(T_c)} \right] [C_2 S(T_c)] N_{N_2} \qquad (12)$$

where $S(T_V)$ is given by equation (9). As with the line intensity method, a room temperature calibration of the band intensity must be performed to determine $[C_2 S(T_c)]$ and the vibrational temperature in the gas must be measured so that the slope ratio $S(T_V)/S(T_c)$ can be obtained. The number density then can be calculated with the band intensity obtained from the test gas and equation (12).

Finally, the number density can be determined by measuring the total intensity of the radiation emitted by the electron beam. However, there are certain difficulties associated with this measurement which do not exist with the others discussed. The total intensity of the N_2^+ radiation is obtained from equation (12) by summing over all values of both v' and v''. The intensity expression obtained can be written in the form

$$I_{N_2^+} = \left[\sum_{v_o} \frac{f(v_o) e^{-G_o(v_o)hc/kT_V}}{Q_{VIB}} \right] N_{N_2} \qquad (13)$$

where $I_{N_2^+}$ denotes the intensity of the N_2^+ emission and $f(v_o)$ is a function of the Franck-Condon factors and wave numbers of the bands. In

addition to the radiation of the N_2^+ system, the emission from the N_2 second positive system also must be included when the total radiation from the beam is considered. While the N_2^+ radiation intensity could be corrected for a varying vibrational temperature, it is unclear how the intensity of the N_2 system relative to that of the N_2^+ system changes with changing vibrational temperature. This may not be a particular difficulty, however, since the (0,0) band of the N_2^+ system is much more intense than any other band in the emission. Radiation from metastable electronic energy states also may be included in the total emissive intensity. The radiation from metastable states is responsible for the "afterglow" observed in flowing gases. Normally, calibration of the total intensity as a function of number density is performed with no gas flow and the calibration then is applied to determine the density in a flowing system. However, the radiation from metastable states included in the intensities of the static calibrations would be swept downstream by the gas flow and out of range of the detector, introducing errors in the density measurement. For nitrogen excited by an electron beam, no significant radiation from metastable states has been observed (see Section IV). For other gases, the possible existence of "afterglow" should be examined before the total radiation intensity is employed for density measurements.

The method chosen for density measurement in any particular situation probably will depend most strongly on the type of spectroscopic equipment available. When there is no vibrational excitation, the total radiation intensity can be employed and a simple photomultiplier tube will suffice as a detector. With vibrational excitation, the total radiation intensity is unsuitable and either a band or line intensity must be used. Further, the vibrational temperature of the radiating species must be measured to obtain an accurate value of the density. Note from Fig. 11 that a 10% error in the band intensity results from ignoring the effects of vibrational excitation at a vibrational temperature of 1500°K. When there is vibrational excitation, the measurement of a band intensity is most readily accomplished with a photomultiplier fitted with an appropriate filter to pass radiation from only one band.

IV. EXPERIMENTAL PROCEDURES

A. ROTATIONAL TEMPERATURE

The rotational temperature must be determined with a spectroscopic instrument with sufficient resolution to separate the rotational lines within a band of the emission. Since the (0,0) band is much more intense than the others, it is employed for rotational temperature measurements. A typical spectrogram obtained with a Baird three-meter grating spectrograph is shown in Fig. 13. This particular instrument has a 15,000 line inch grating with a linear dispersion of 5.6 angstroms per millimeter in

the first order. With a 100 micron entrance slit width, the fine structure of the (0,0) band is just resolved.

Various types of spectroscopic plates were examined for use with the Baird spectrograph and Kodak type 103a-0 were found to require the shortest exposure time. With the electron beam passing through air at a pressure of 200 μ Hg at room temperature, an exposure time of 20 minutes was required to obtain a moderate photographic density on the plates.

The intensities of the rotational lines are determined with a recording micro-densitometer. A typical trace from the densitometer for the (0,0) band is shown in Fig. 14. As an example of rotational temperature determination, the analysis of the trace shown in Fig. 14 will be discussed.

The first step in the analysis is to determine the relationship between relative intensity and photographic density for the plate emulsion. Various standard calibration techniques are available.[1] In this case, the relative intensity of a line from a standard source is assumed equal to the exposure time. The intensity calibration is obtained by plotting exposure time against the densitometer reading as shown in Fig. 15. The scatter of data points evident in Fig. 15 results primarily from the grainy nature of the 103a-0 emulsion.

The densitometer readings obtained for each line from the trace of Fig. 14 are tabulated below.

TABLE 1

TYPICAL LINE INTENSITIES FOR $N_2^+(0,0)$ BAND

K'	Densitometer Reading	I/I_o	$\text{Log}_{10}[(G)(\nu^4/\nu_o^4)K']$	$\text{Log}_{10}[I/I_o^1/(G)(\nu^4/\nu_o^4)K']$
3	62	2.70	0.471	-.040
4	79	1.80	0.597	-.041
5	39	3.73	0.695	-.123
6	73	2.13	0.775	-.146
7	31	4.25	0.842	-.214
8	70	2.30	0.901	-.238
9	29	4.50	0.954	-.301
10	70	2.30	1.002	-.339
11	33	4.10	1.044	-.431
12	76	1.96	1.083	-.490
13	42	3.57	1.120	-.567
14	81	1.69	1.153	-.623
15	55	2.98	1.185	-.711

The relative intensities corresponding to the densitometer readings are obtained from the intensity calibration, Fig. 15. The values of $\log_{10}[G\nu^4/\nu_o^4]$ are determined from Table 3 for an estimated temperature of 400°K and $\log_{10}[K'G\nu^4/\nu_o^4]$ is calculated for each line. Now, because of the homonuclear structure of the N_2^+ molecule, lines with odd values of K' appear with intensities which are twice those of the lines with even K' values. Hence, the intensities of lines with even K' values were doubled before calculating $\log_{10}\left[\frac{I/I_o}{K'G\nu^4/\nu_o^4}\right]$. The rotational temperature is determined by plotting this intensity function against $K'(K'+1)$ as shown in Fig. 16. The slope of the straight line in Fig. 16 yields a temperature of 418°K. Since this temperature is slightly different from the assumed value of 400°K, new values of $\log_{10}[K'G\nu^4/\nu_o^4]$ could be obtained from Table 3 and the temperature re-determined by iteration. In the present case, the correction in the assumed temperature will not alter the final result.

Detailed experimental studies reported in Refs. 3 and 4 substantiate the validity of the above procedures. Considering the possibility for systematic photometric errors, the accuracy of the rotational temperature is judged to be ± 3%.

B. VIBRATIONAL TEMPERATURE

As discussed in Section III, the vibrational temperature of the N_2 molecules is determined by measuring the intensity of various bands in the emission. For this purpose, a spectroscopic device which separates the bands must be employed. In these studies, a Bausch and Lomb f/5 quartz prism spectrograph was used. A typical spectrogram obtained with this instrument is shown in Fig. 17 where only radiation from the N_2^+ first negative and N_2 second positive systems is evident. Note in particular the absence of any radiation from metastable energy states or species other than N_2. Kodak type 103a-F spectroscopic plates give optimum results with the Bausch and Lomb spectrograph at exposure times equal to 3.5 minutes for an air pressure of 200 μ Hg at room temperature.

A typical densitometer trace for the (0,2) band of the N_2^+ emission is shown in Fig. 18. Calibration data relating the relative intensity to photographic density must be placed on the plate as discussed in the previous section. The band intensity is determined by numerically integrating with wavenumber the intensity values obtained from the densitometer readings and the intensity calibration. This integration procedure is conducted for all bands with suitable intensities. Since many bands are present in the spectrum, the vibrational temperature can be determined separately from many band intensity ratios and the curves of Fig. 10.

A practical difficulty which exists, however, is the determination of the wavelength dependence of the emulsion sensitivity. In order to compare

the intensities of bands in different spectral regions, the change in the relative sensitivity of the emulsion over the wavelength range must be determined. This requires a light source with a radiation output calibrated as a function of wavelength and very careful experimental procedures. The wavelength sensitivity calibration can be avoided, however, by comparing the intensities of bands only within a given band progression. That is, compare the intensities of the (0,2), (1,3) and (2,4) bands or those of the (0,1), (1,2), and (2,3) bands. Since bands of a progression are separated by only approximately 60 Å, the neglect of the change of emulsion sensitivity over the length of a progression will not introduce serious errors.

As an example of vibrational temperature determination, various band intensity ratios and the corresponding vibrational temperatures are tabulated below. The tabulated data were obtained with an electron beam and an arc-heated wind tunnel operating with air as the effluent and are reproduced below from Table 2 of Ref. 4. The band intensities were determined by integration as discussed above.

TABLE 2

N_2 VIBRATIONAL TEMPERATURES DETERMINED WITH AN ELECTRON BEAM

Distance from Tunnel ℄ Transverse to Flow in Inches	I_{01}/I_{12}	I_{12}/I_{23}	I_{01}/I_{23}	Ave.
-1.0	2350	2820	2600	2590
- .50	2720	2700	2700	2706
+ .25	3000	2550	2800	2783
+ .50	3150	2230	2430	2603
+ .75	2420	2250	2320	2330
+1.0	2000	1850	1900	1916

The obvious source of error in vibrational temperature measurements is inaccuracy in the various values for the Franck-Condon factors employed in the band intensity ratio expression. These Franck-Condon factors probably are not known to better than 5-10%. Further, the method of data reduction can introduce sizable errors. Spectral regions of a band away from the band head (Fig. 18) contribute a sizable amount to the intensity. However, the inherent grainy nature of the photographic emulsion is most noticeable with low intensities and causes errors in the contributions of the weaker portions of the band. Considering the various sources of error, the vibrational temperature accuracy by this method is probably no better than ± 15%. The scatter of the temperatures in Table 2 is approximately ± 5% around the average value for each row.

Photographic procedures certainly are not the most convenient for vibrational temperature measurements. Most scanning monochromaters have sufficient resolution to separate the band structure and direct intensity values can be obtained from a photomultiplier attached to the monochrometer. In this case, only the spectral response of the photomultiplier need be determined to obtain accurate data.

A further simplification in the detection system can be achieved by simply employing two or more photomultipliers fitted with narrow bandpass filters so that each photomultiplier "sees" radiation from only one band. Calibrations of the relative sensitivities of the photomultipliers will yield corrected band intensities for use with Fig. 10. A vibrational temperature accuracy of ± 5% should be possible with more direct measuring techniques.

C. NUMBER DENSITY

As discussed in Section III-E, the N_2 number density may be determined in a variety of ways. The validity of all of the methods depends upon the linearity of the variation of the measured intensity with N_2 number density. Nonlinearity of the variation results principally from collision quenching of the excited nitrogen ions. The amount of quenching depends upon the concentration of quenching particles and the collision cross section for the interaction between the quenching particle and the excited ion. Since the amount of quenching depends upon the concentrations of the quenching particles, it would be extremely difficult to apply a non-linear room temperature calibration in an effluent where the detailed chemical composition is unknown. In Ref. 4, detailed experimental studies were conduted to determine the effects of quenching on the various density measurements. It was found that for the maximum densities examined (corresponding to a pressure of 400 μ Hg at room temperature), quenching was evident in neither rotational line nor vibrational band intensities.

The variation of the intensity with N_2 number density of the $K' = 11$ line in the N_2^+ (0,0) band reproduced from Ref. 4 is shown in Fig. 19. The slope of this curve is equal to the factor $[C_1 S(T_c) R(T_c)]$ in equation (11). To increase the accuracy of the line intensity determination, the quantity $\log_{10}[(I/I_o)/K'G\nu^4/\nu_o^4]$ was plotted versus $K'(K'+1)$ and the smoothed value of the logarithm was used to calculate the line strength. To determine the N_2 density from the calibration (Fig. 19) and the smoothed line strength obtained from the test condition, both the rotational and vibrational temperatures must be measured so that the slope correction factors can be determined (Fig. 11 and 12). With the slope ratios $S(T_V)/S(T_c)$ and $R(T_R)/R(T_c)$ and the room temperature slope $[C_1 S(T_c) R(T_c)]$, the variation of $I_{K',K''}$ versus N_{N_2} corrected for vibrational and rotational temperatures different from those of the calibration can be obtained.

A sample calibration of the intensity of the $N_2^+(0,0)$ band is shown in Fig. 20. In this case, a 1P28 photomultiplier tube fitted with a

Farrand interference filter was used. The filter allowed radiation only from the (0,0) band to strike the photocathode. The slope of the photomultiplier output versus N_2 number density constitutes the factor $C_2S(T_c)$ in equation (12). Again, this calibration curve must be corrected for a vibrational temperature (but not rotational temperature) difference between the test and calibration conditions. This is accomplished by measuring the vibrational temperature and referring to Fig. 11. Note that this technique is particularly simple when there is no vibrational excitation in the test condition so that the slope ratio $S(T_V)/S(T_c)$ is unity.

When there is vibrational excitation of the test gas, the vibrational temperature must be determined. The band intensities employed for vibrational temperature measurement also can be utilized for density measurement. Typical calibrations of the N_2^+ (0,2) and (1,2) band intensities obtained with the Bausch and Lomb spectrograph are shown in Fig. 21. The procedure for density measurement with this type of calibration is identical to that discussed above for the photomultiplier application.

The common cause of error in density measurement with an electron beam is due to a slight change in the alignment of the beam and optical system between calibration and test exposures. Particular care must be exercised to assure that this does not occur so that the sensitivity of the detecting system remains unchanged. This is particularly bothersome when testing with an arc-heated wind tunnel since small changes in the strength of the ambient magnetic field can cause deflections of the beam and subsequent misalignment of the beam-optical system. It should be noted that these sensitivity changes will not affect the temperature measurements, since only relative intensities are employed rather than the "absolute" intensities of the density measurements.

V. SUMMARY AND CONCLUSION

An electron beam device suitable for use with low density nonradiating flows has been described. The beam can be utilized for direct measurements of the rotational and vibrational temperatures and concentrations of nitrogen molecules present in a high speed air flow. The technique can be applied regardless of the gasdynamic nature of the flow (i.e., in boundary layers, shock layers, wakes, etc.). The beam causes no noticeable disturbance of the test gas and in this regard has proven to be a powerful flow diagnostic device.

The electron beam system presently in use at The Ohio State University has been described and certain design criteria have been specified. A wide variety of optical equipment can be employed for the measurements and experimental data obtained with various spectrographs and photomultipliers has been presented for illustrative purposes.

The theoretical analyses required for interpretation of the beam data have been summarized. The pertinent quantities utilized in data reduction procedures have been presented in tabular form and sample calculations have been discussed.

The electron beam technique should be examined further to determine the maximum flow density which can be examined before collision quenching of the radiation becomes an important factor. Application of the technique to species other than nitrogen also should be investigated.

REFERENCES

1. Fishburne, E. S. and Petrie, S. L.; "Spectrographic Analysis of Plasma Flows;" Dept. of Aero-Astro. Engr., The Ohio State University; ASD Tech. Documentary Rept. ASD-TDR-63-98, 1963.

2. Gadamer, E. O.; "Application of an Electron Gun to Density Measurements in Rarefied Gas Flow;" UTIA Bulletin and Progress Report, 1960.

3. Muntz, E. P.; "Measurement of Rotational Temperature, Vibrational Temperature, and Molecule Concentration in Non-Radiating Flows of Low Density Nitrogen;" University of Toronto Inst. of Aerophysics Rept. 71, April, 1961.

4. Petrie, S. L., Pierce, G. A., and Fishburne, E. S.; "Analysis of the Thermo-Chemical State of an Expanded Air Plasma;" Dept. of Aero-Astro. Engr., The Ohio State University; ASD Tech. Documentary Rept. AFFDL-TR-64-191, December, 1964.

5. MacArthur, R. C., et al; "Flow Visualization and Quantitative Gas Density Measurements in Rarefied Gas Flows;" ASD-TDR-62-793, December, 1962.

6. Laurmann, J. E. (Editor;) Rarefied Gas Dynamics, Vol. II; Academic Press, New York, 1903.

7. Herzberg, G.; Spectra of Diatomic Molecules; D. van Nostrand and Co., New York, 1950.

TABLE 3

VALUES OF $\log_{10}[(G)\nu^4/\nu_0^4]$ FOR VARIOUS ROTATIONAL TEMPERATURES

(Reproduced from Ref. 3)

K' / T_{ROT} °K	3	5	7	9	11	13	15	17	19	21
75	-.018	.006	.037	.078	.124	.175	.231	.290	.351	.414
100	-.016	-.003	.016	.041	.069	.107	.136	.175	.217	.260
125	-.015	-.005	.007	.023	.043	.064	.089	.116	.146	.177
150	-.013	-.006	.003	.014	.028	.044	.062	.082	.104	.128
175	-.011	-.007	0	.009	.019	.032	.045	.061	.078	.097
200	-.011	-.006	-.001	.006	.014	.024	.035	.047	.001	.076
225	-.010	-.006	-.002	.004	.011	.019	.028	.038	.050	.061
250	-.009	-.006	-.002	.003	.009	.015	.022	.031	.041	.051
300	-.007	-.005	-.003	.001	.006	.010	.016	.022	.030	.037
373	-.006	-.004	-.003	0	.003	.007	.011	.015	.021	.026
400	-.006	-.004	-.003	0	.003	.006	.009	.014	.019	.024
450	-.005	-.003	-.002	0	.003	.005	.008	.012	.016	.020
500	-.005	-.003	-.002	0	.002	.005	.007	.010	.014	.017
550	-.004	-.003	-.002	0	.002	.004	.006	.009	.012	.016
600	-.004	-.003	-.002	0	.002	.004	.006	.009	.012	.014
700	-.003	-.002	-.001	0	.002	.003	.005	.007	.010	.012
800	-.003	-.002	-.001	0	.002	.003	.005	.007	.009	.012
900	-.003	-.002	-.001	0	.002	.003	.005	.006	.009	.011
1.000	-.002	-.001	-.001	.001	.002	.003	.004	.006	.009	.010

TABLE 4

WAVELENGTHS OF VIBRATIONAL BANDS FOR
$N_2^+ B^2\Sigma \rightarrow N_2^+ X^2\Sigma$ IN ANGSTROMS

v"\v'	0	1	2	3	4
0	3914	3582	3308		
1	4278	3884	3564	3299	
2	4709	4236	3858	3549	3293
3	5228	4652	4199	3835	3538
4	5865	5149	4600	4167	3818

TABLE 5

RELATIVE VIBRATIONAL TRANSITION PROBABILITIES

$p(v',v'') = R_e^2 q(v',v'')$

FOR TRANSITION $N_2^+B^2\Sigma \rightarrow N_2^+X^2\Sigma$

(Reproduced from Ref. 3)

$v'\backslash v''$	0	1	2	3	4
0	.54	.23	.07	.02	
1	.21	.21	.27	.26	.05
2	.04	.29	.06	.23	.17

TABLE 6

FRANCK-CONDON FACTORS FOR TRANSITION $N_2^+B^2\Sigma \rightarrow N_2^+X^2\Sigma$

(Reproduced from Ref. 3)

$v'\backslash v''$	0	1	2
0	.65	.26	$.07_4$
1	.30	.22	.29
2	$.04_7$	.41	$.04_3$
3	$.00_3$	.11	.43

TABLE 7

FRANCK-CONDON FACTORS FOR TRANSITION $N_2X^1\Sigma \rightarrow N_2^+B^2\Sigma$

(Reproduced from Ref. 3)

$v'\backslash v_0$	0	1	2
0	.90	$.08_6$	$.00_9$
1	$.09_5$	.74	.14
2	$.00_1$	.17	.63

TABLE 8

RELATIVE POPULATIONS OF $N_2 X^1\Sigma$ VIBRATIONAL ENERGY LEVELS, $e^{-G_o(v_o)hc, kTv}$

$T_v(^oK)\backslash v_o$	0	1	2	3	4	5	6	7	8	9	10	Q_{VIB}
500	1	.001	$<10^{-4}$	$<10^{-4}$	$<10^{-4}$	$<10^{-4}$	$<10^{-4}$	$<10^{-4}$				1.00
750	1	.011	$<10^{-4}$	$<10^{-4}$	$<10^{-4}$	$<10^{-4}$	$<10^{-4}$	$<10^{-4}$				1.01
1000	1	.035	.001	$<10^{-4}$	$<10^{-4}$	$<10^{-4}$	$<10^{-4}$	$<10^{-4}$				1.04
1250	1	.068	.005	$<10^{-3}$	$<10^{-4}$	$<10^{-4}$	$<10^{-4}$	$<10^{-4}$				1.07
1500	1	.107	.012	$<10^{-3}$	$<10^{-3}$	$<10^{-4}$	$<10^{-4}$	$<10^{-4}$				1.12
1750	1	.147	.022	.003	$<10^{-3}$	$<10^{-3}$	$<10^{-4}$	$<10^{-4}$				1.17
2000	1	.187	.035	.007	.001	$<10^{-3}$	$<10^{-3}$	$<10^{-4}$				1.23
2250	1	.225	.051	.012	.003	$<10^{-3}$	$<10^{-3}$	$<10^{-3}$				1.29
2500	1	.262	.069	.019	.005	.002	$<10^{-3}$	$<10^{-3}$				1.36
2750	1	.295	.082	.027	.008	.003	$<10^{-3}$	$<10^{-3}$				1.42
3000	1	.327	.108	.036	.012	.004	.001	$<10^{-3}$				1.49
3250	1	.356	.128	.047	.017	.006	.002	$<10^{-3}$	$<10^{-3}$			1.56
3500	1	.384	.148	.058	.023	.009	.004	.002	$<10^{-3}$	$<10^{-3}$		1.63
3750	1	.409	.169	.071	.030	.013	.006	.002	.001	$<10^{-3}$		1.70
4000	1	.433	.188	.083	.037	.017	.008	.004	.002	$<10^{-3}$		1.77
4250	1	.454	.208	.096	.045	.022	.010	.005	.002	.001	$<10^{-3}$	1.84
4500	1	.474	.228	.110	.053	.026	.013	.007	.003	.002	$<10^{-3}$	1.92
4750	1	.494	.247	.124	.063	.032	.017	.009	.005	.002	.001	1.99
5000	1	.512	.265	.137	.072	.038	.020	.011	.006	.003	.002	2.07

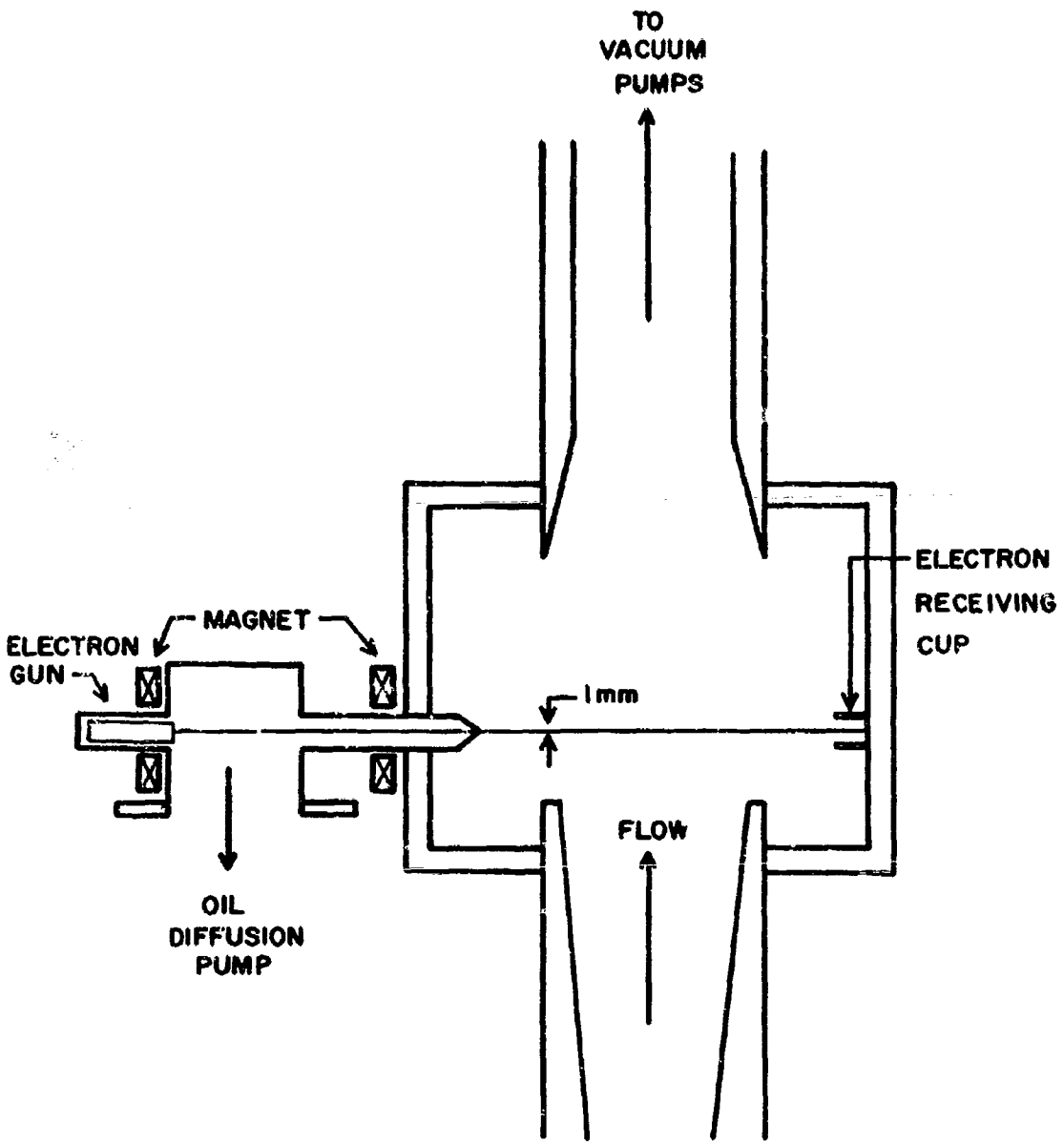

FIGURE 1

ELECTRON BEAM SCHEMATIC

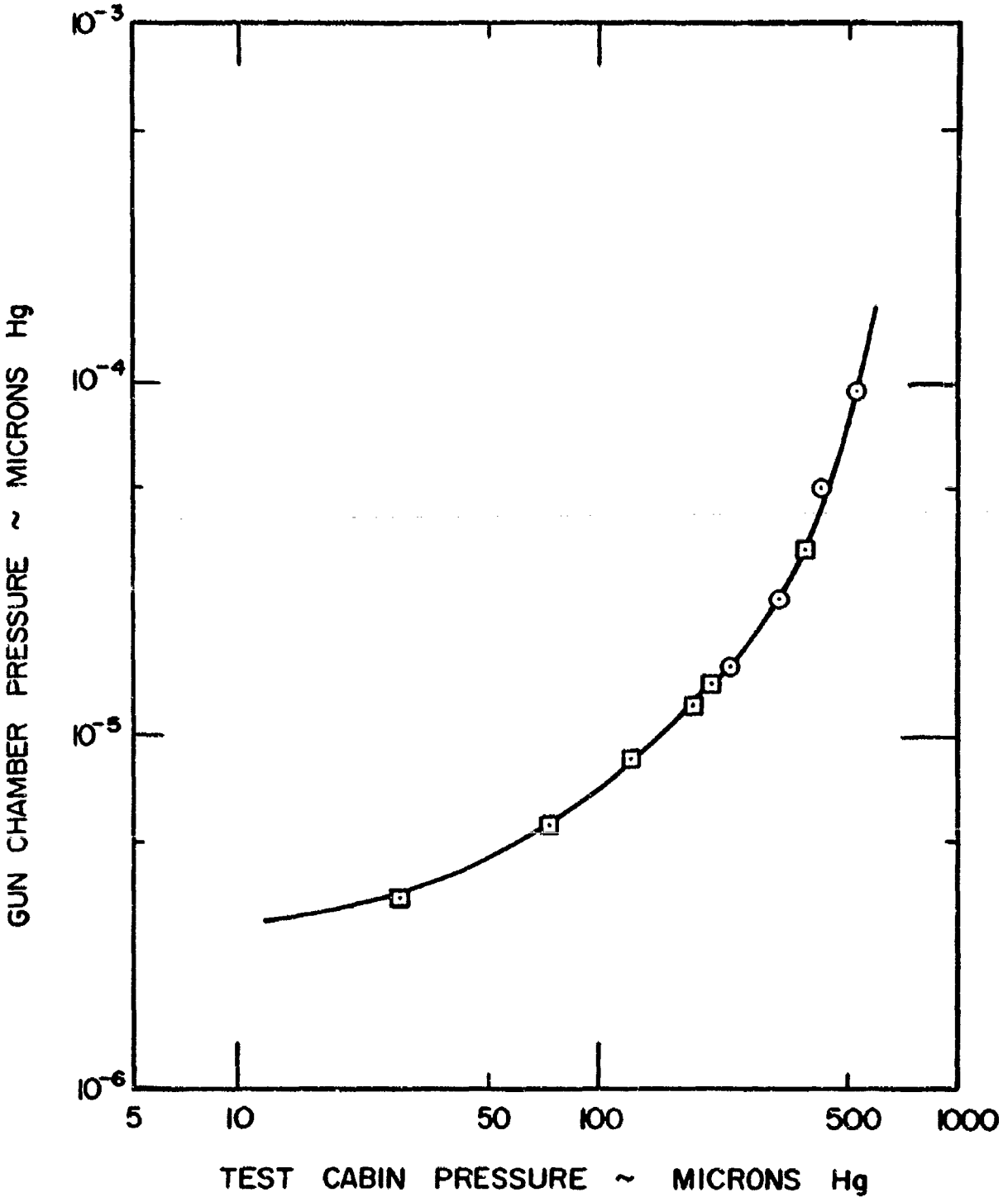

FIGURE 2

ELECTRON BEAM VACUUM SYSTEM PERFORMANCE

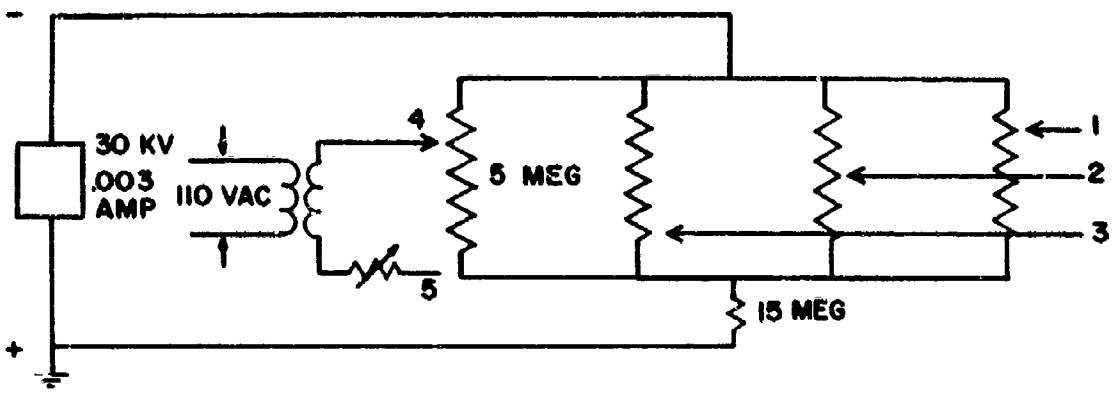

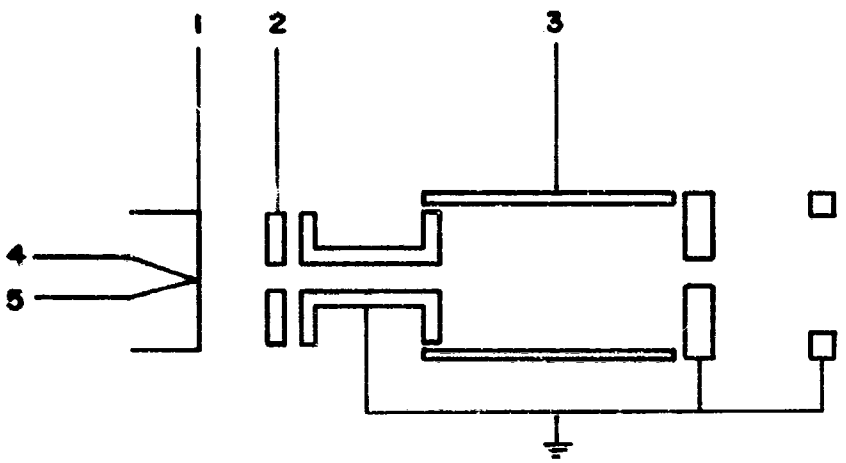

19BWP4 ELECTRON GUN

FIGURE 3

ELECTRON GUN SCHEMATIC

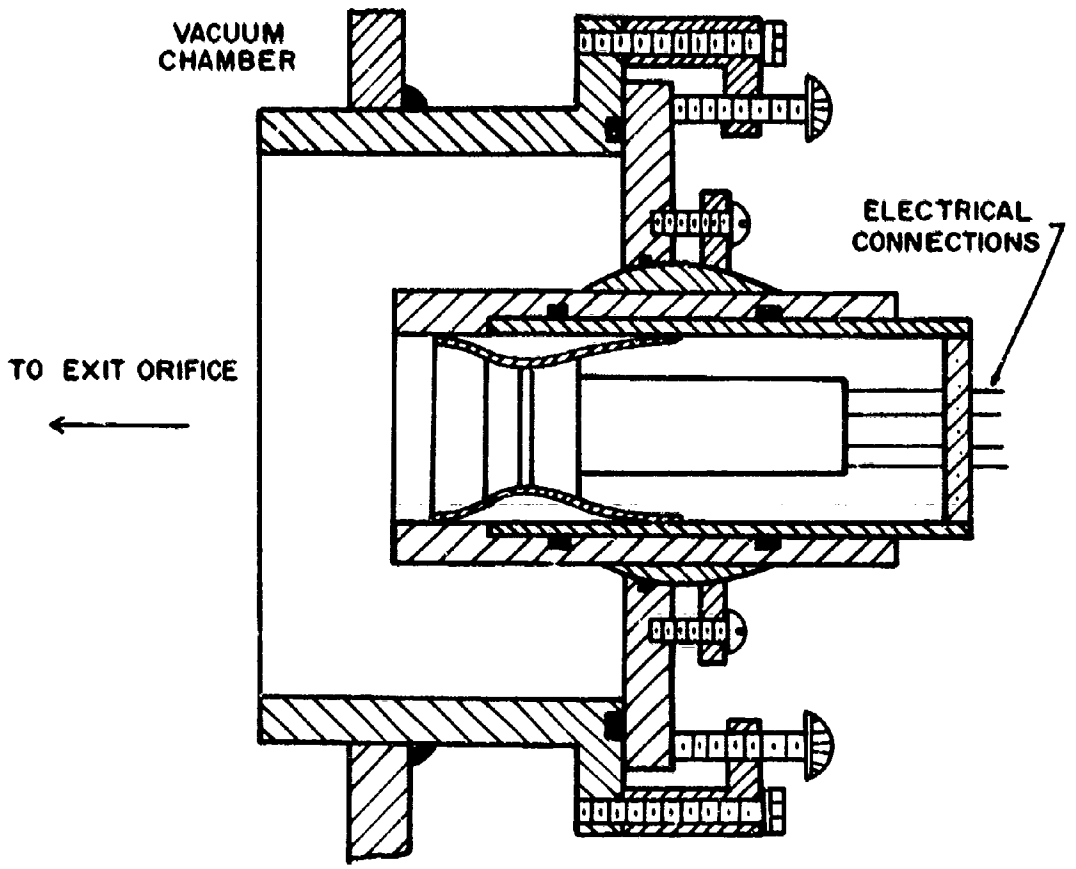

FIGURE 4

GUN MOUNT DETAILS

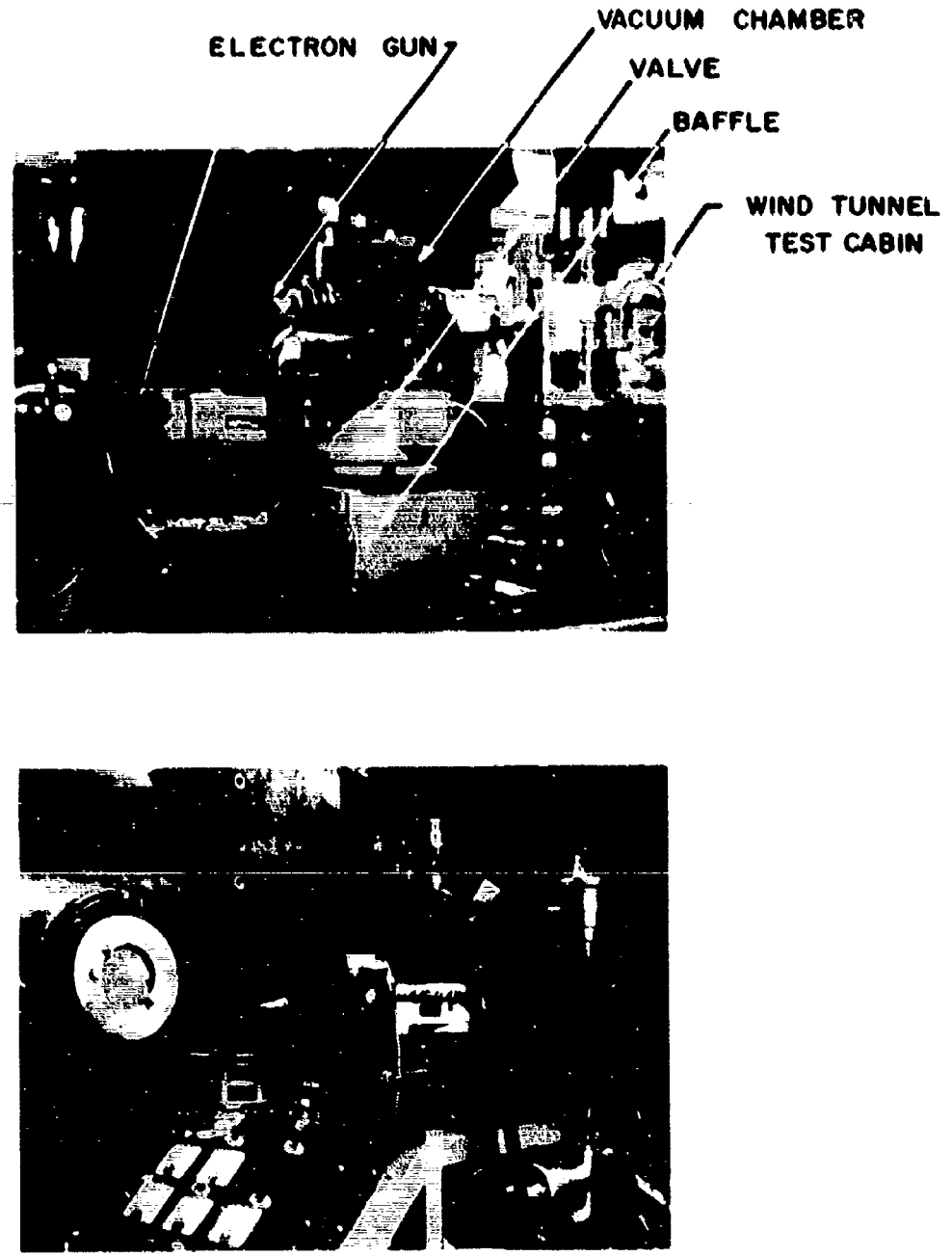

FIGURE 5

ELECTRON BEAM GENERATORS

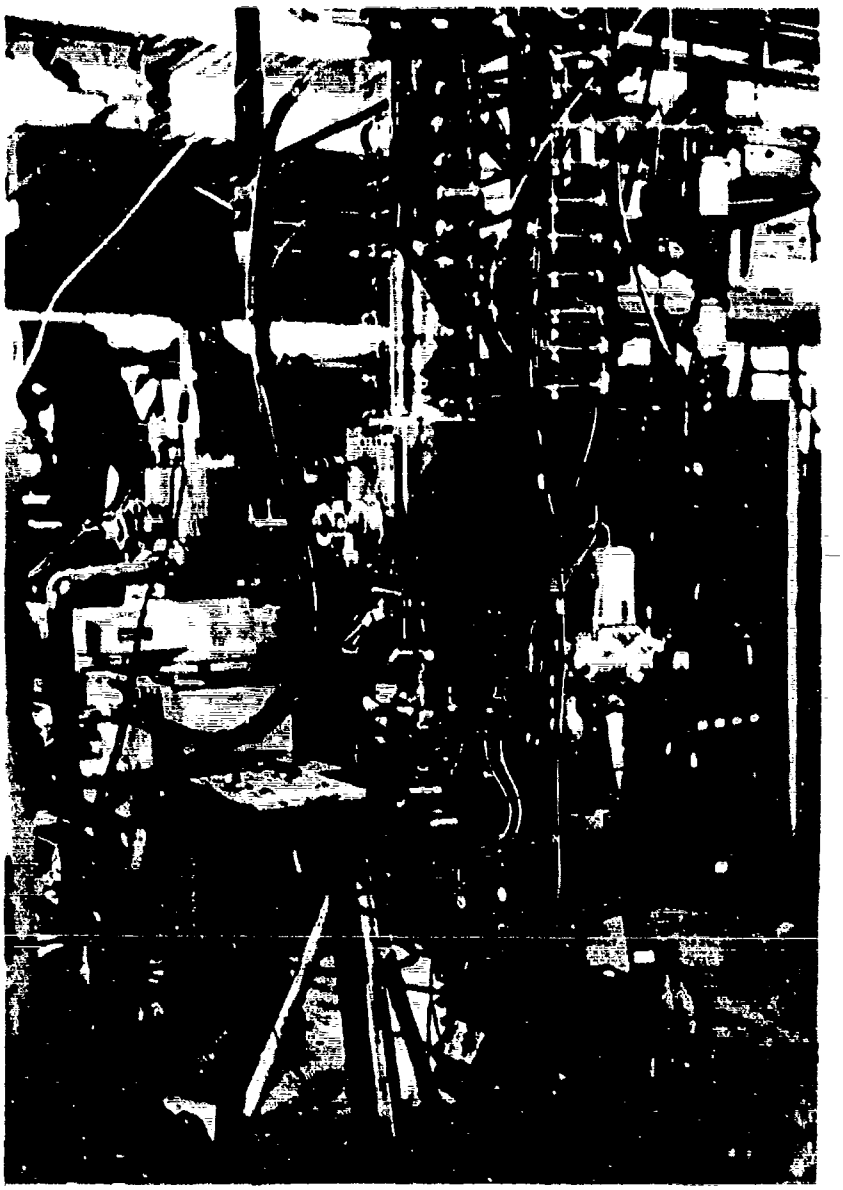

FIGURE 6

BEAM—WIND TUNNEL ASSEMBLY

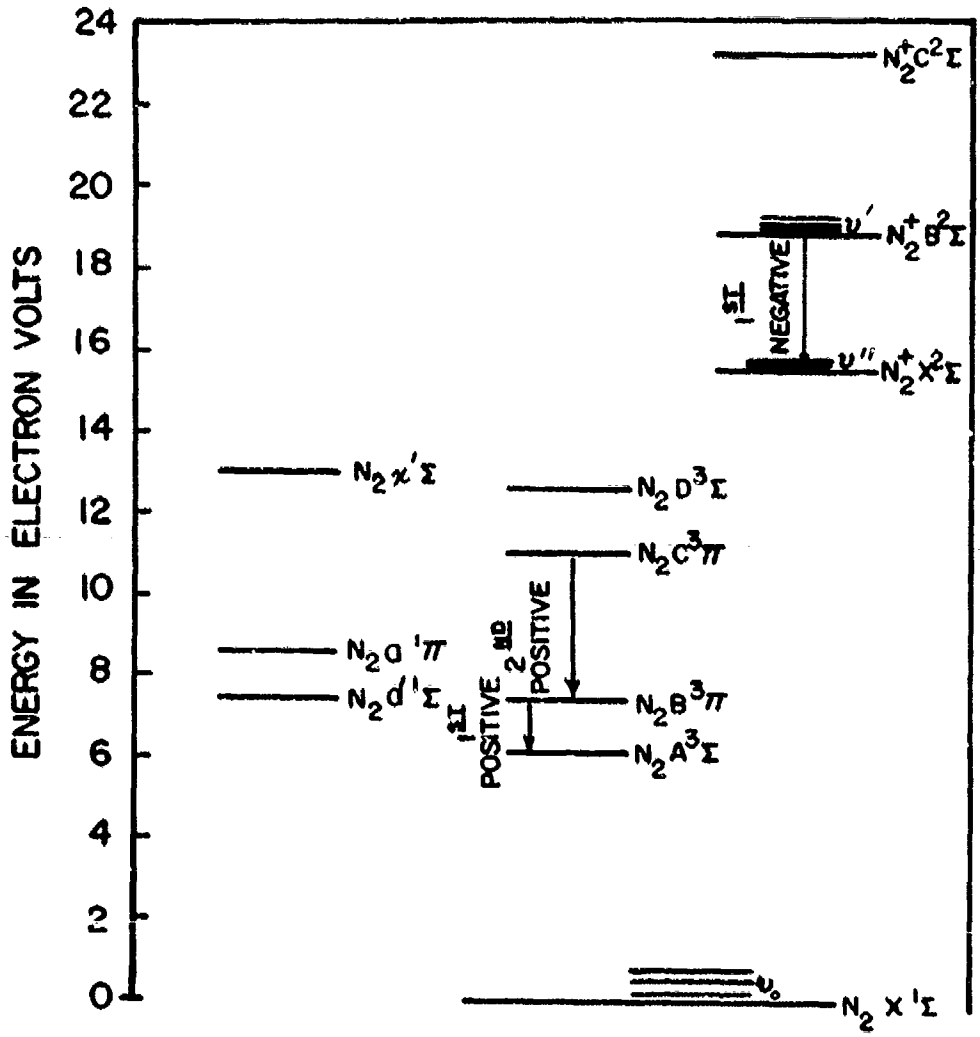

FIGURE 7

PARTIAL ENERGY LEVEL DIAGRAM FOR N_2 AND N_2^+

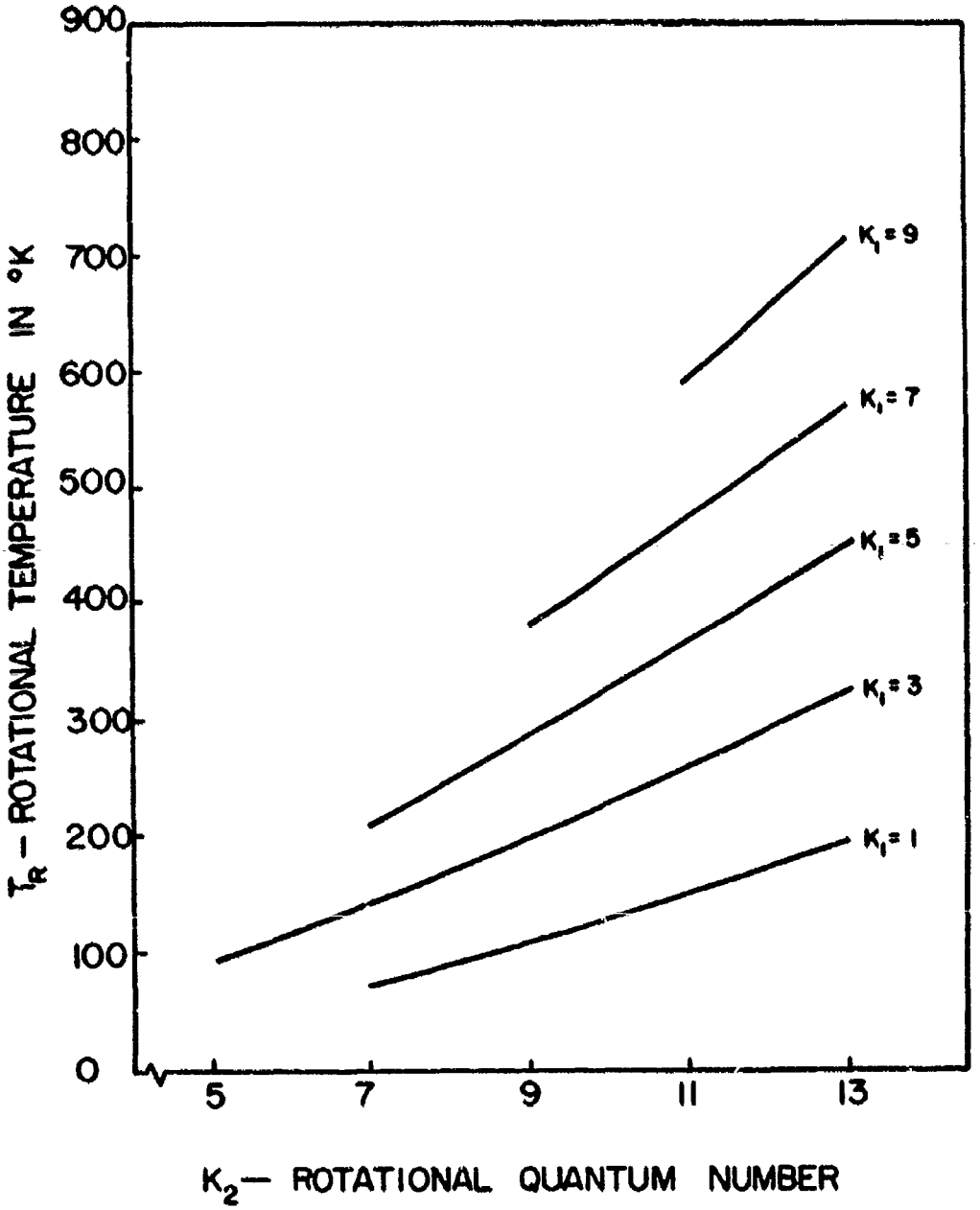

FIGURE 8

ISO—INTENSITY PLOT FOR (0,0) BAND OF N_2^+ FIRST NEGATIVE EMISSION; T_R versus K_2

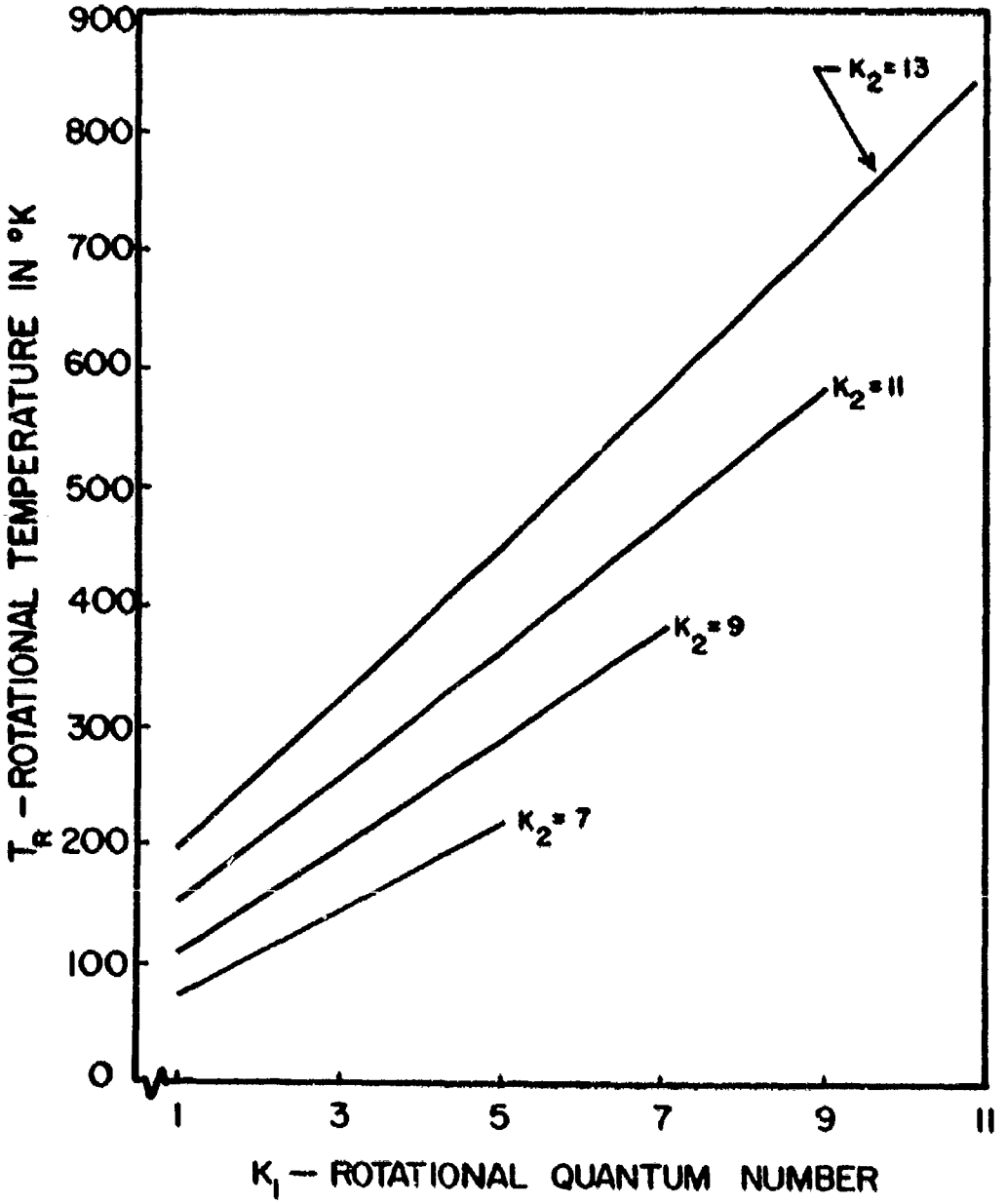

FIGURE 9

ISO–INTENSITY PLOT FOR (0,0) BAND OF N_2^+ FIRST NEGATIVE EMISSION ; T_R versus K_1

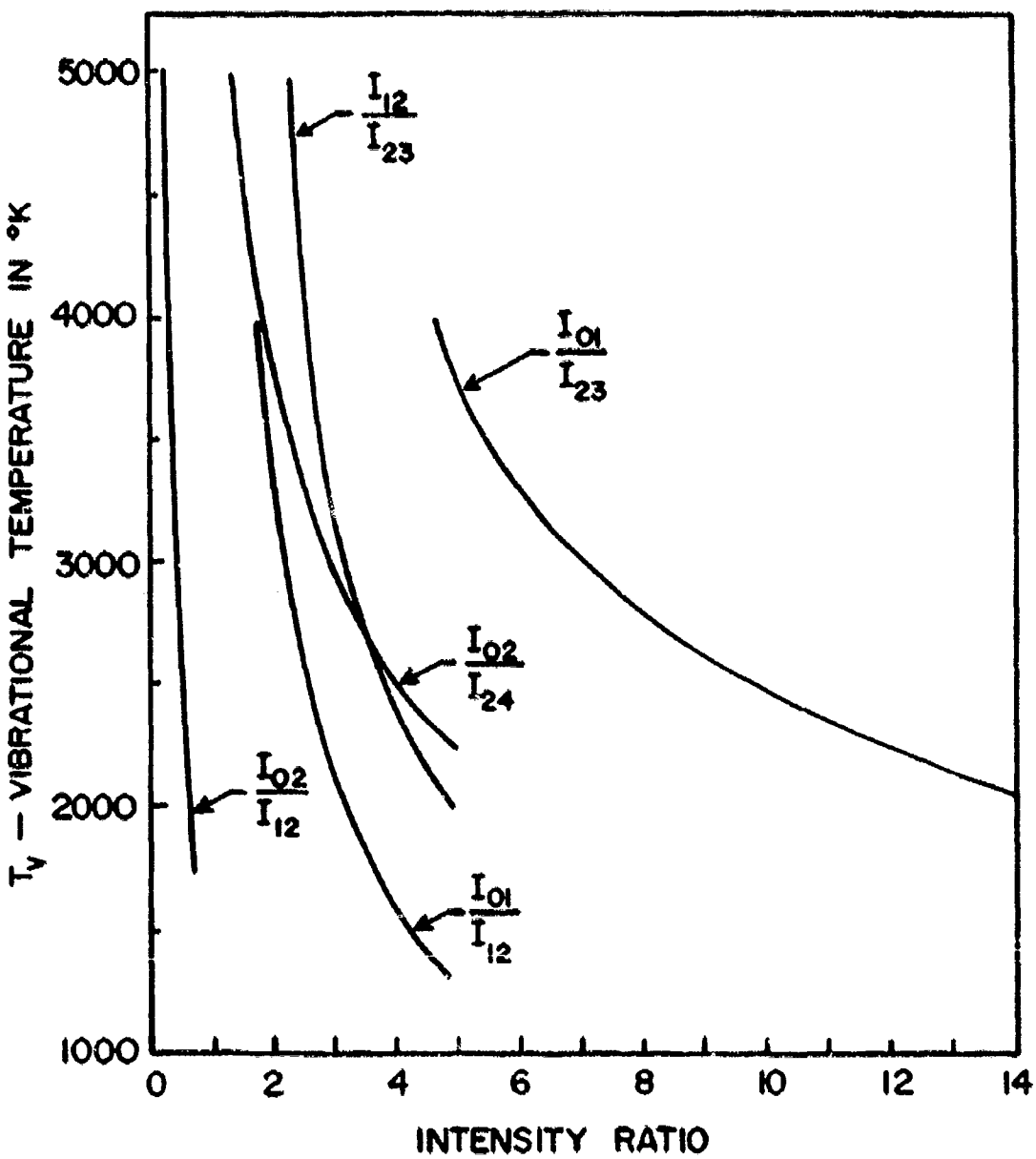

FIGURE 10

BAND INTENSITY RATIOS FOR N_2^+ FIRST NEGATIVE EMISSION SYSTEM

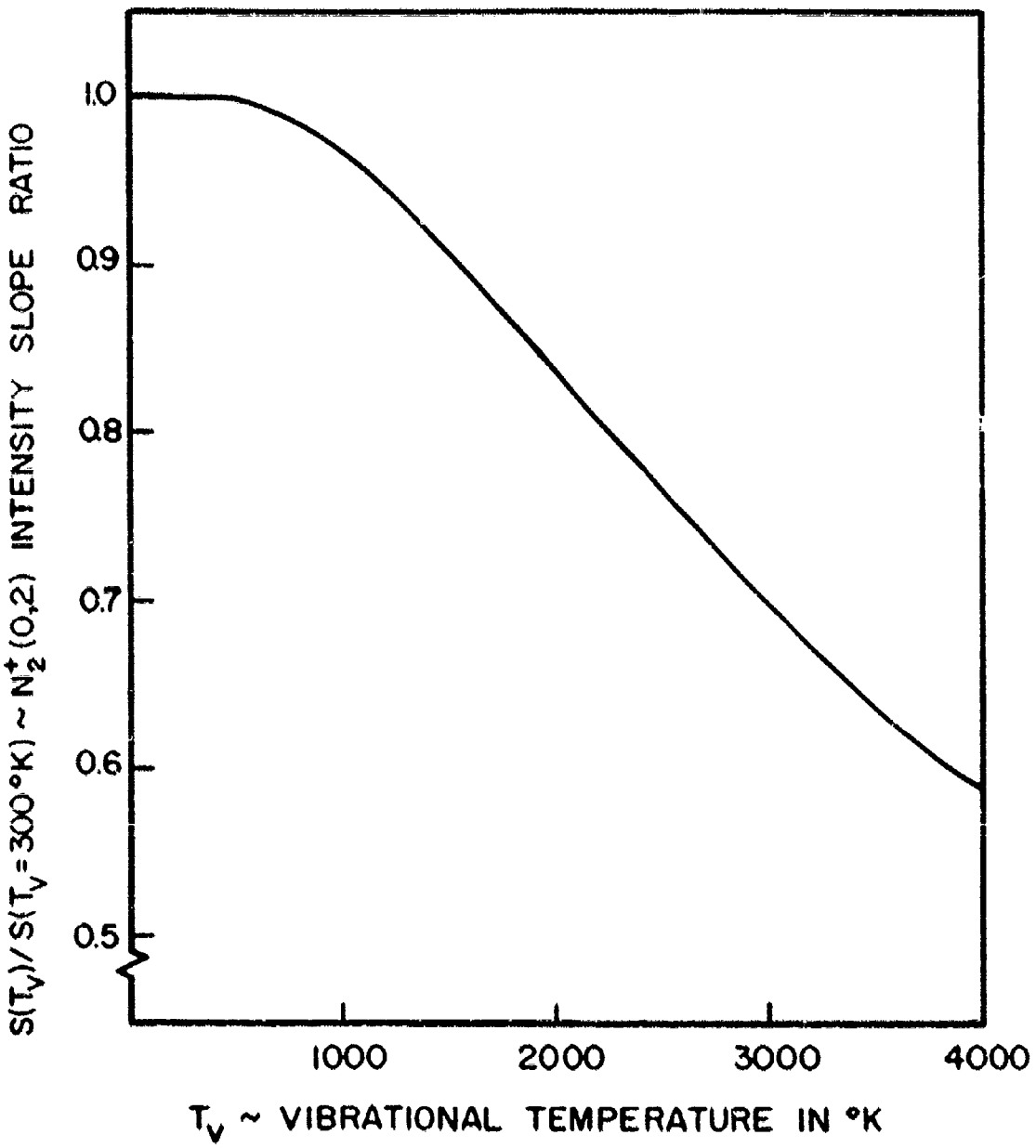

FIGURE 11

$N_2^+(0,2)$ BAND INTENSITY SLOPE RATIO AS A FUNCTION OF VIBRATIONAL TEMPERATURE

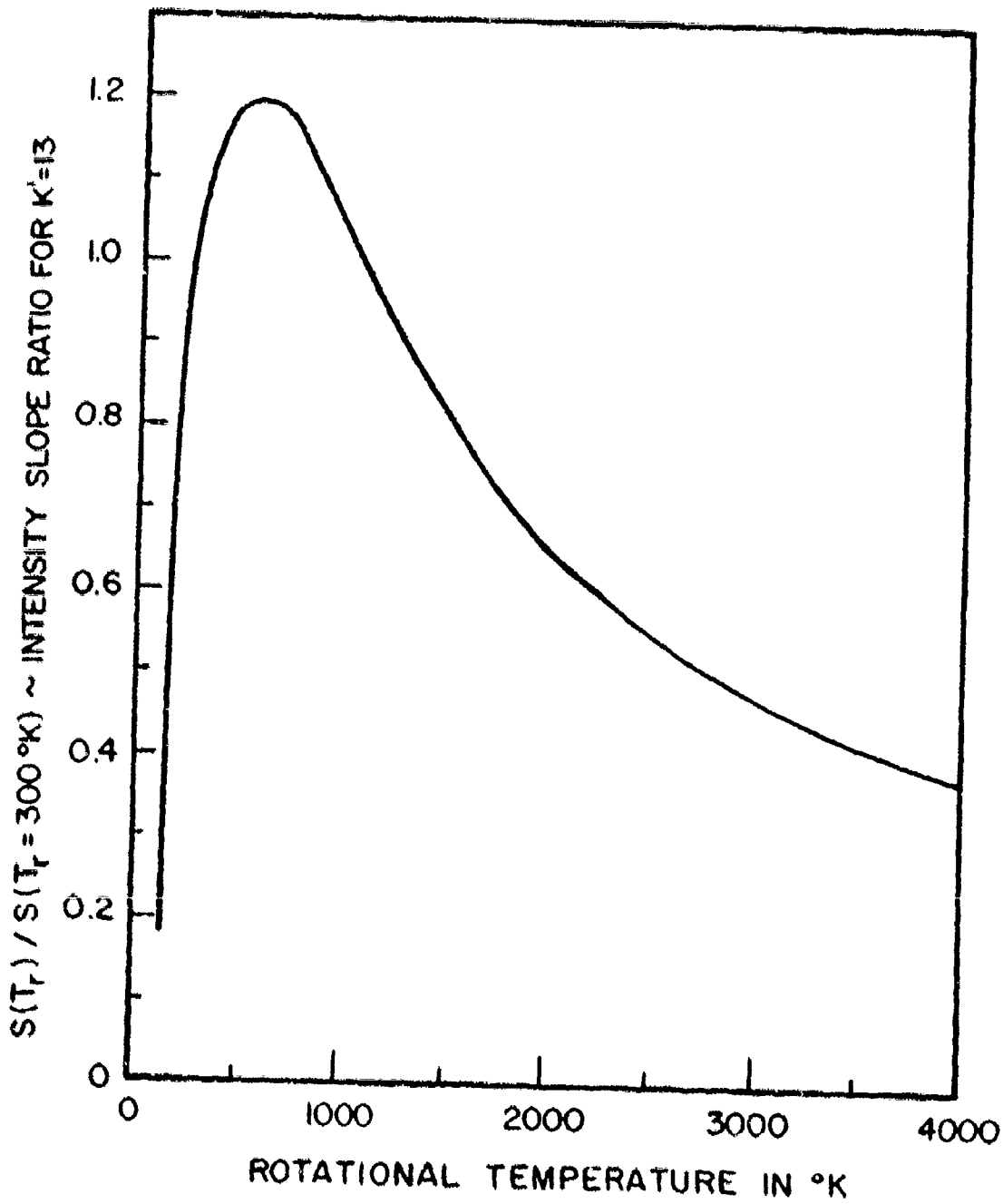

FIGURE 12

K'=13 LINE INTENSITY SLOPE RATIO AS A FUNCTION OF ROTATIONAL TEMPERATURE

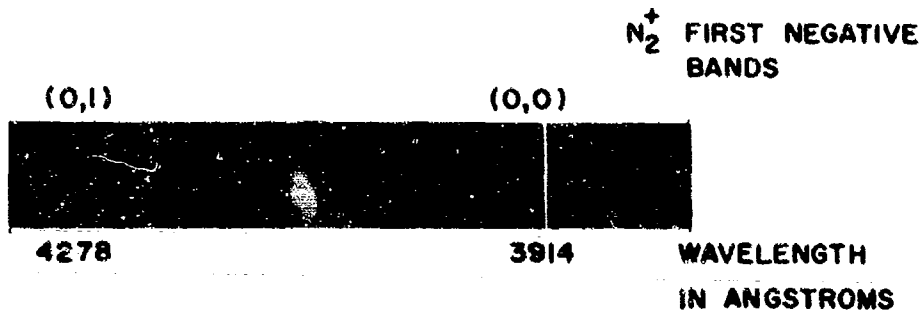

FIGURE 13

TYPICAL SPECTROGRAM FROM 3-METER GRATING SPECTROGRAPH

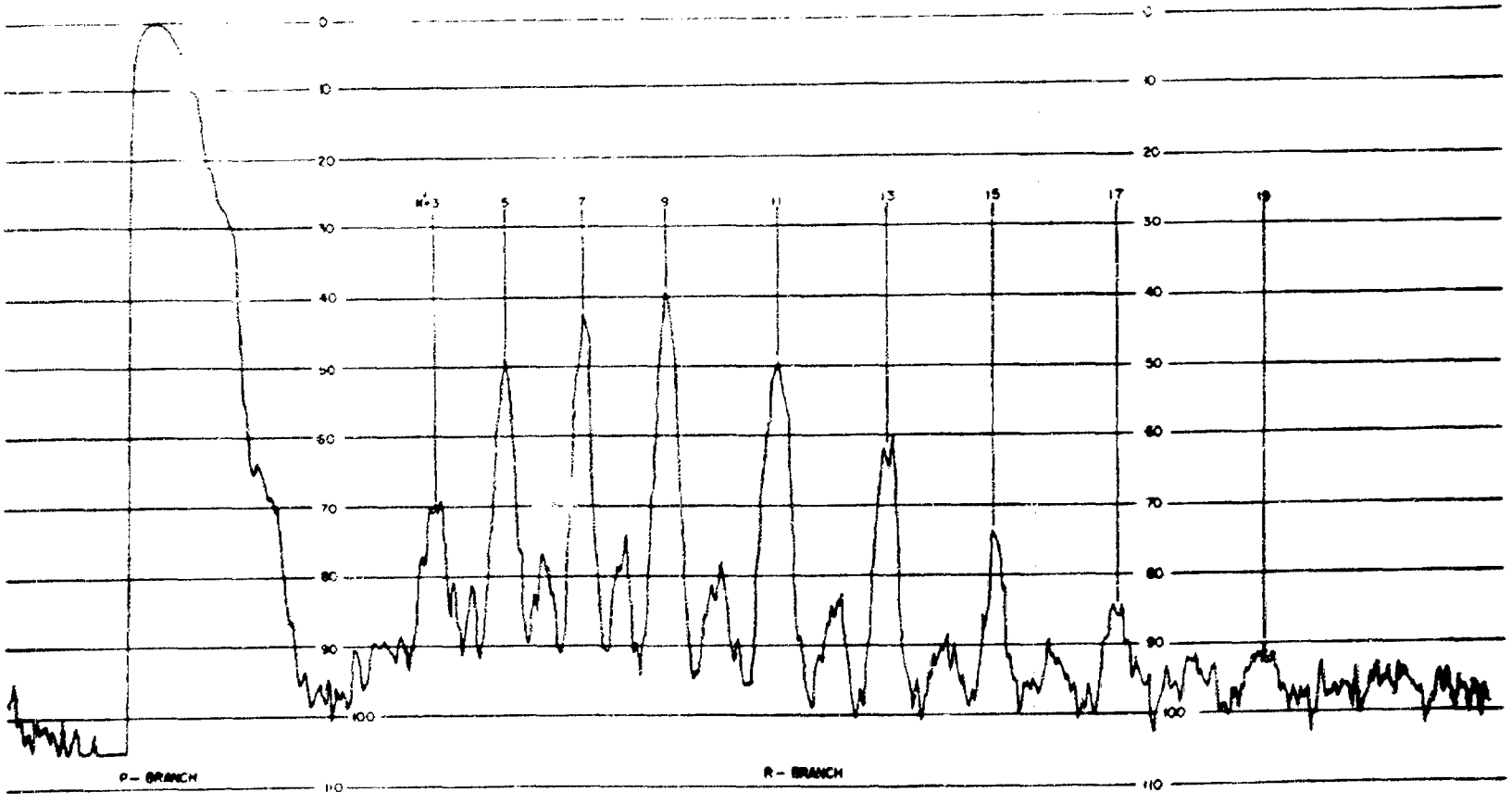

FIGURE 14

DENSITOMETER RECORDING FOR N_2^+ (0,0) BAND

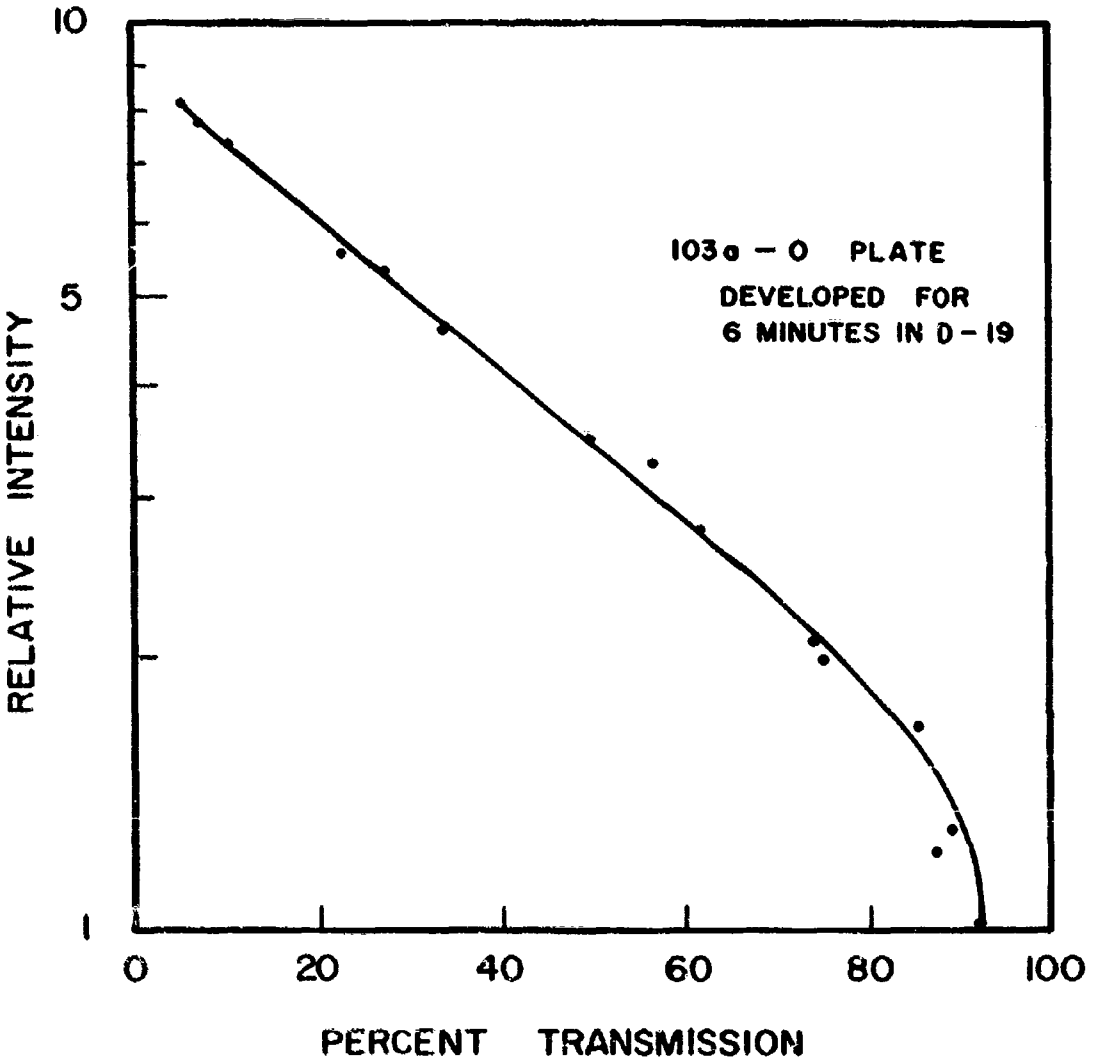

FIGURE 15

TYPICAL EMULSION CALIBRATION

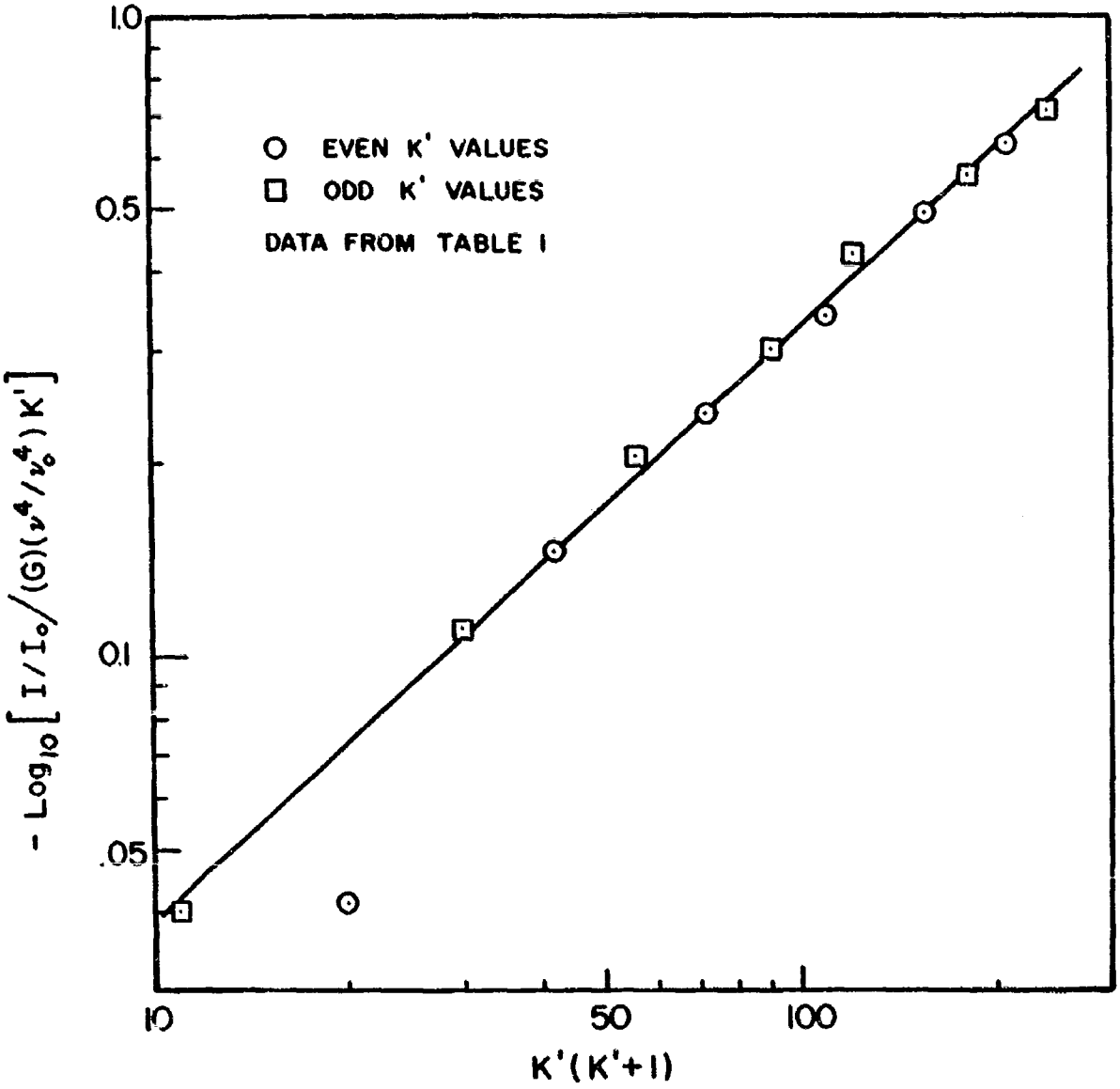

FIGURE 16

LINE–SLOPE PLOT FOR N_2^+ (0,0) BAND

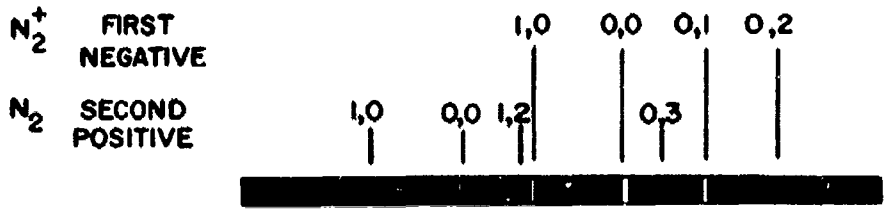

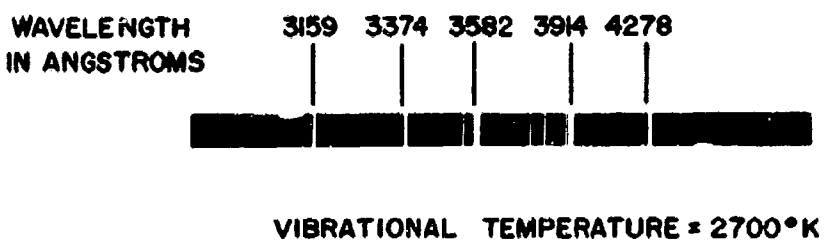

FIGURE 17

TYPICAL SPECTROGRAMS FROM f/5 PRISM SPECTROGRAPH

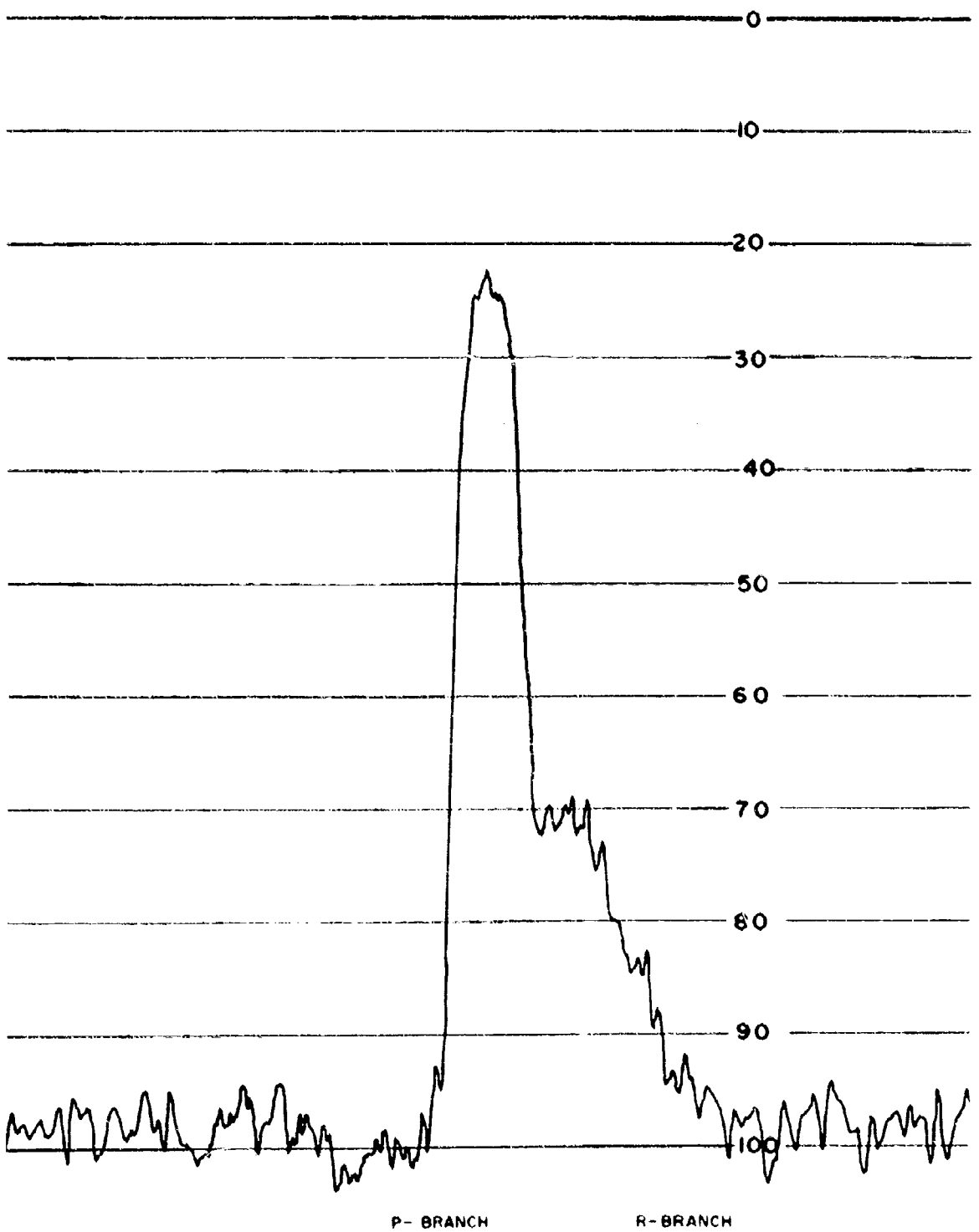

FIGURE 18

DENSITOMETER TRACE OF N_2^+ (0,2) BAND

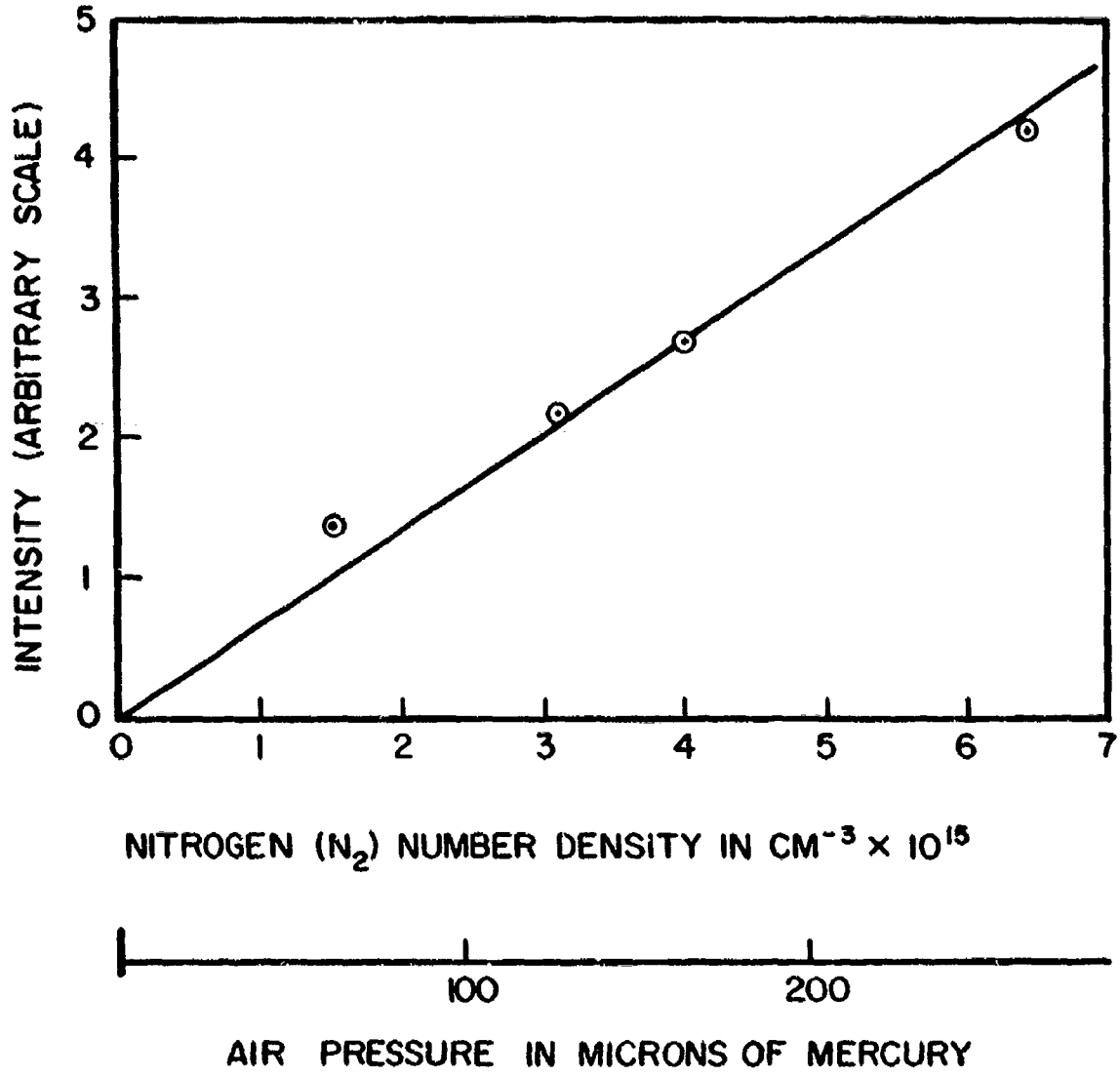

FIGURE 19

K'= 11 LINE INTENSITY IN N_2^+ (0,0) BAND DETERMINED WITH A SPECTROGRAPH AS A FUNCTION OF N_2 NUMBER DENSITY AT ROOM TEMPERATURE

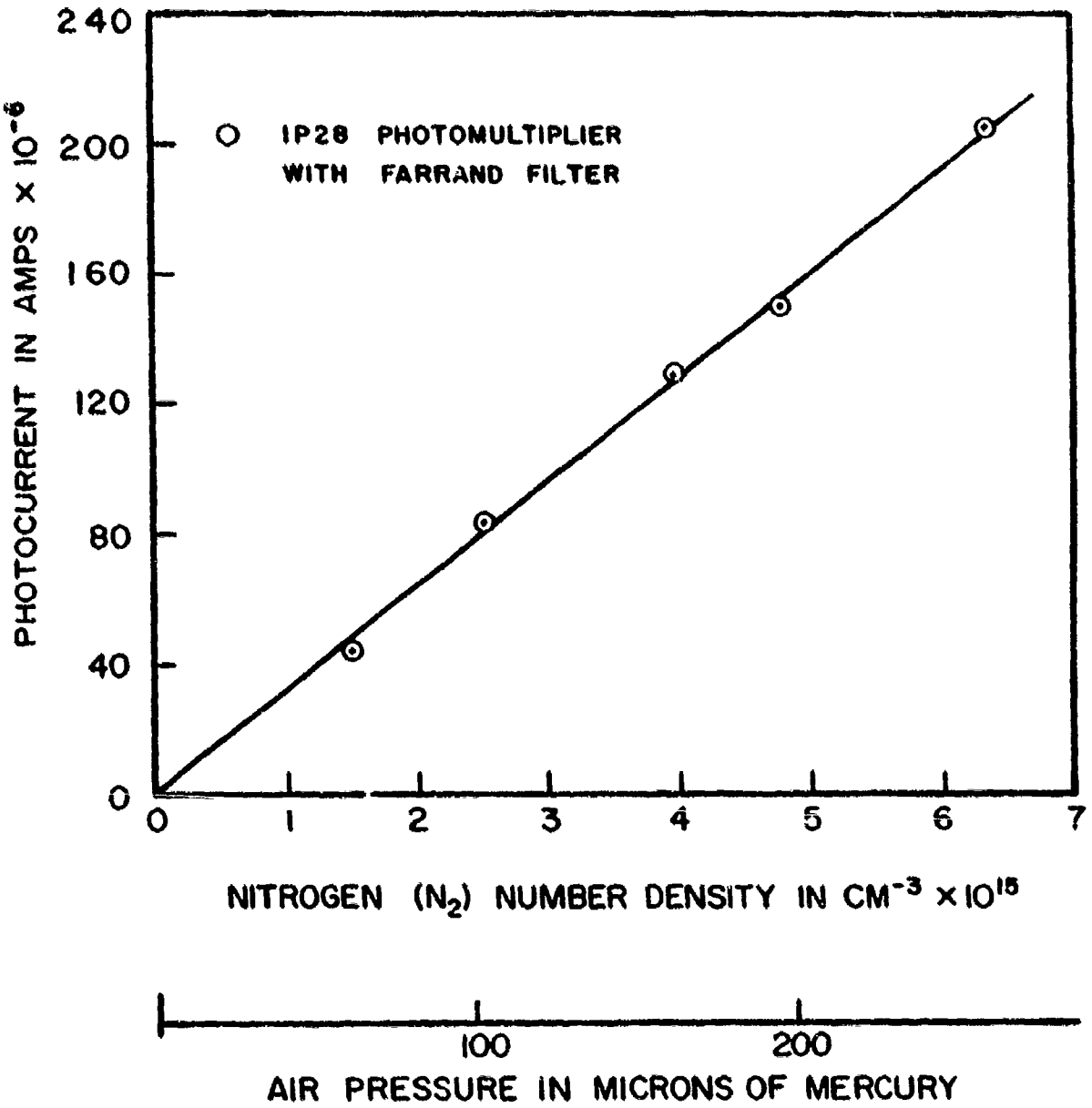

FIGURE 20

N_2^+ (0,0) BAND INTENSITY DETERMINED WITH A PHOTOMULTIPLIER AS A FUNCTION OF N_2 NUMBER DENSITY AT ROOM TEMPERATURE

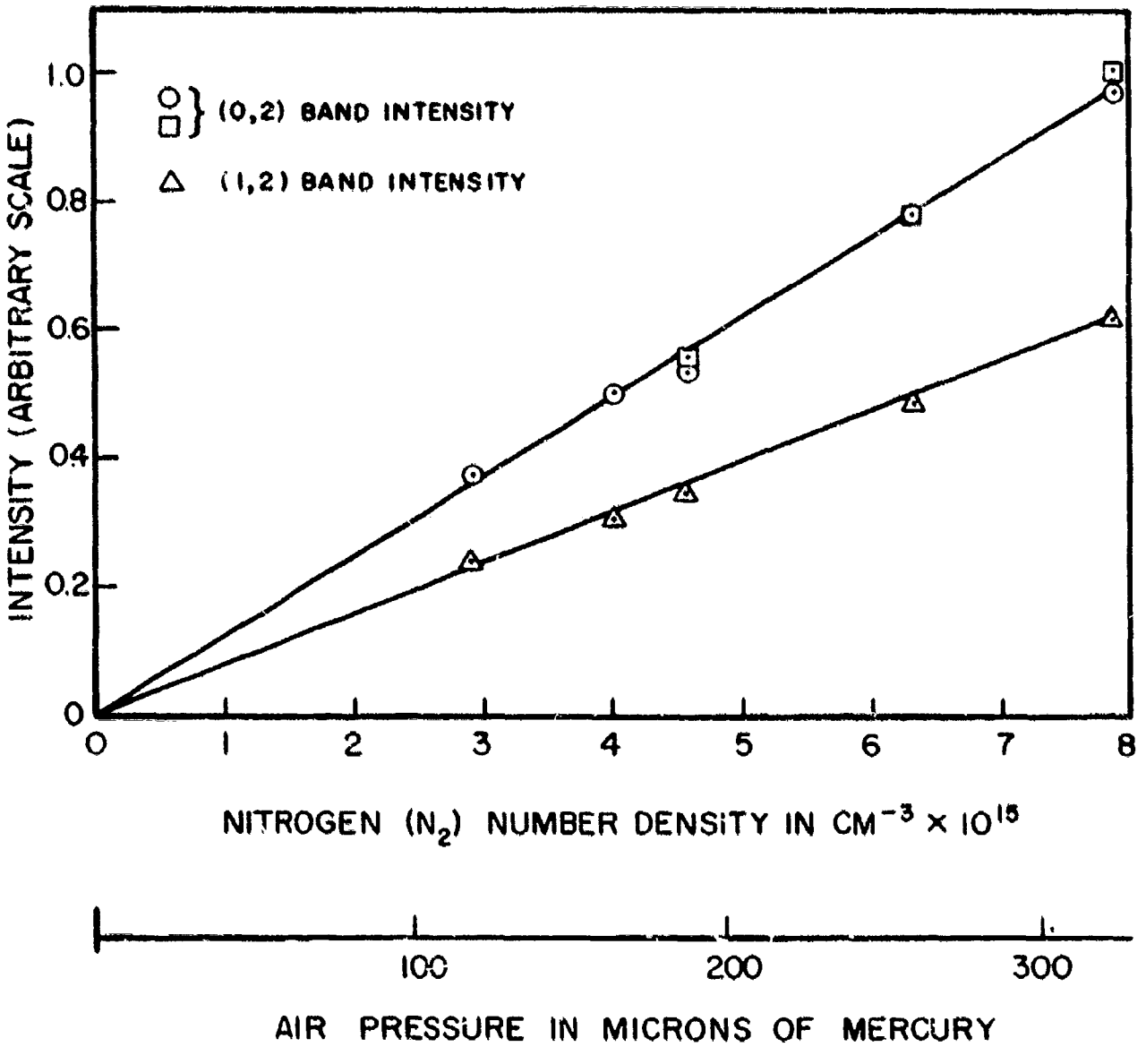

FIGURE 21

N_2^+ (0,2) AND (1,2) BAND INTENSITIES DETERMINED WITH A PRISM SPECTROGRAPH AS A FUNCTION OF N_2 NUMBER DENSITY AT ROOM TEMPERATURE

Unclassified

Security Classification

DOCUMENT CONTROL DATA - R&D

(Security classification of title, body of abstract and indexing annotation must be entered when the overall report is classified)

1 ORIGINATING ACTIVITY (Corporate author)
The Ohio State University Research Foundation
1314 Kinnear Road, Columbus, Ohio

2a REPORT SECURITY CLASSIFICATION
Unclassified

2b GROUP

3 REPORT TITLE
An Electron Beam Device for Real Gas Flow Diagnostics

4 DESCRIPTIVE NOTES (Type of report and inclusive dates)
Interim Report

5 AUTHOR(S) (Last name, first name, initial)
Petrie, S. L.

6 REPORT DATE	7a TOTAL NO. OF PAGES	7b NO. OF REFS
June 1965	50	7

8a CONTRACT OR GRANT NO.	9a ORIGINATOR'S REPORT NUMBER(S)
AF 33(657)-11060	Technical Report No. 1
b PROJECT NO. 7065	
c	9b OTHER REPORT NO(S) (Any other numbers that may be assigned this report)
d	ARL 65-122

10 AVAILABILITY/LIMITATION NOTICES
Qualified requesters may obtain this report from DDC.
Copies available from OTS.

11 SUPPLEMENTARY NOTES	12 SPONSORING MILITARY ACTIVITY
	Aerospace Research Laboratories Office of Aerospace Research, USAF Wright-Patterson AFB, Ohio

13 ABSTRACT

An electron beam device suitable for use in low density, non-radiating flows is described. It is shown that in certain ranges of gas density the electron beam can be employed to determine the rotational temperature, vibrational temperature and concentration of molecular nitrogen in a high speed air flow. The theoretical analysis required for interpretation of the data obtained with an electron beam is presented and examples of application of the technique are given. Certain design criteria for electron beam generators are discussed.

DD FORM 1 JAN 64 1473

Unclassified

Unclassified
Security Classification

14 KEY WORDS	LINK A		LINK B		LINK C	
	ROLE	WT	ROLE	WT	ROLE	WT
Electron beams Flow diagnostics						

INSTRUCTIONS

1. ORIGINATING ACTIVITY: Enter the name and address of the contractor, subcontractor, grantee, Department of Defense activity or other organization *(corporate author)* issuing the report.

2a. REPORT SECURITY CLASSIFICATION: Enter the overall security classification of the report. Indicate whether "Restricted Data" is included. Marking is to be in accordance with appropriate security regulations.

2b. GROUP: Automatic downgrading is specified in DoD Directive 5200.10 and Armed Forces Industrial Manual. Enter the group number. Also, when applicable, show that optional markings have been used for Group 3 and Group 4 as authorized.

3. REPORT TITLE: Enter the complete report title in all capital letters. Titles in all cases should be unclassified. If a meaningful title cannot be selected without classification, show title classification in all capitals in parenthesis immediately following the title.

4. DESCRIPTIVE NOTES: If appropriate, enter the type of report, e.g., interim, progress, summary, annual, or final. Give the inclusive dates when a specific reporting period is covered.

5. AUTHOR(S): Enter the name(s) of author(s) as shown on or in the report. Enter last name, first name, middle initial. If military, show rank and branch of service. The name of the principal author is an absolute minimum requirement.

6. REPORT DATE: Enter the date of the report as day, month, year, or month, year. If more than one date appears on the report, use date of publication.

7a. TOTAL NUMBER OF PAGES: The total page count should follow normal pagination procedures, i.e., enter the number of pages containing information.

7b. NUMBER OF REFERENCES: Enter the total number of references cited in the report.

8a. CONTRACT OR GRANT NUMBER: If appropriate, enter the applicable number of the contract or grant under which the report was written.

8b, &, & 8d. PROJECT NUMBER: Enter the appropriate military department identification, such as project number, subproject number, system numbers, task number, etc.

9a. ORIGINATOR'S REPORT NUMBER(S): Enter the official report number by which the document will be identified and controlled by the originating activity. This number must be unique to this report.

9b. OTHER REPORT NUMBER(S): If the report has been assigned any other report numbers *(either by the originator or by the sponsor)*, also enter this number(s).

10. AVAILABILITY LIMITATION NOTICES: Enter any limitations on further dissemination of the report, other than those imposed by security classification, using standard statements such as:

(1) "Qualified requesters may obtain copies of this report from DDC."

(2) "Foreign announcement and dissemination of this report by DDC is not authorized."

(3) "U. S. Government agencies may obtain copies of this report directly from DDC. Other qualified DDC users shall request through _____."

(4) "U. S. military agencies may obtain copies of this report directly from DDC. Other qualified users shall request through _____."

(5) "All distribution of this report is controlled. Qualified DDC users shall request through _____."

If the report has been furnished to the Office of Technical Services, Department of Commerce, for sale to the public, indicate this fact and enter the price, if known.

11. SUPPLEMENTARY NOTES: Use for additional explanatory notes.

12. SPONSORING MILITARY ACTIVITY: Enter the name of the departmental project office or laboratory sponsoring *(paying for)* the research and development. Include address.

13. ABSTRACT: Enter an abstract giving a brief and factual summary of the document indicative of the report, even though it may also appear elsewhere in the body of the technical report. If additional space is required, a continuation sheet shall be attached.

It is highly desirable that the abstract of classified reports be unclassified. Each paragraph of the abstract shall end with an indication of the military security classification of the information in the paragraph, represented as *(TS)*, *(S)*, *(C)*, or *(U)*.

There is no limitation on the length of the abstract. However, the suggested length is from 150 to 225 words.

14. KEY WORDS: Key words are technically meaningful terms or short phrases that characterize a report and may be used as index entries for cataloging the report. Key words must be selected so that no security classification is required. Identifiers, such as equipment model designation, trade name, military project code name, geographic location, may be used as key words but will be followed by an indication of technical context. The assignment of links, roles, and weights is optional.